Preparation of Tris-Heteroleptic Iridium(III) Complexes Containing a Cyclometalated Aryl-NHC Ligand

Vadim Adamovich,[b] Sonia Bajo,[a] Pierre-Luc T. Boudreault,[b] Miguel A. Esteruelas,[a] Ana M. López,[a] Jaime Martín,[a] Montserrat Oliván,[a] Enrique Oñate,[a] Adrián U. Palacios,[a] Ainhoa San-Torcuato,[a] Jui-Yi Tsai,[b] and Chuanjun Xia[b]*

[a]Departamento de Química Inorgánica – Instituto de Síntesis Química y Catálisis Homogénea (ISQCH) – Centro de Innovación en Química Avanzada (ORFEO-CINQA), Universidad de Zaragoza – CSIC, 50009 Zaragoza, Spain

[b]Universal Display Corporation, 375 Phillips Boulevard, Ewing, New Jersey 08618, USA

Supporting Information.

ABSTRACT. A new class of phosphorescent tris-heteroleptic iridium(III) complexes has been discovered. Addition of PhMeImAgI (PhMeIm = 1-phenyl-3-methylimidazolylidene) to the dimer [Ir(μ-Cl)(COD)]$_2$ (**1**; COD = 1,5-cyclooctadiene) affords IrCl(COD)(PhMeIm) (**2**), which reacts with 1-phenylisoquinoline, 2-phenylpyridine, and 2-(2,4-difluorophenyl)pyridine to give the respective dimers [Ir(μ-Cl){κ^2-*C*,*C*-(C$_6$H$_4$-ImMe)}{κ^2-*C*,*N*-(C$_6$H$_4$-isoqui)}]$_2$ (**3**), [Ir(μ-Cl){κ^2-

C,*C*-(C_6H_4-ImMe)}{κ^2-*C*,*N*-(C_6H_4-py)}]$_2$ (**4**), and [Ir(μ-Cl){κ^2-*C*,*C*-(C_6H_4-ImMe)}{κ^2-*C*,*N*-($C_6F_2H_2$-py)}]$_2$ (**5**), as a result of the NHC- and N-heterocycle-supported *ortho*-CH bond activation of the aryl substituents and the hydrogenation of a C-C double bond of the coordinated diene. In solution, these dimers exist as a mixture of isomers **a** (Im *trans* to N) and **b** (Im *trans* to Cl), which lie in a dynamic equilibrium. Treatment of **3**, **4**, and **5** with Kacac (acac = acetylacetonate) yields isomers **a** (Im *trans* to N) and **b** (Im *trans* to O) of Ir{κ^2-*C*,*C*-(C_6H_4-ImMe)}{κ^2-*C*,*N*-(C_6H_4-isoqui)}(κ^2-*O*,*O*-acac) (**6a** and **6b**), Ir{κ^2-*C*,*C*-(C_6H_4-ImMe)}{κ^2-*C*,*N*-(C_6H_4-py)}(κ^2-*O*,*O*-acac) (**7a** and **7b**), and Ir{κ^2-*C*,*C*-(C_6H_4-ImMe)}{κ^2-*C*,*N*-($C_6F_2H_4$-py)}(κ^2-*O*,*O*-acac) (**8a** and **8b**), which were separated by column chromatography. Treatment of **6a** with HX in acetone-water produces the protonation of the acac ligand and the formation of the bis(aquo) complex [Ir{κ^2-*C*,*C*-(C_6H_4-ImMe)}{κ^2-*C*,*N*-(C_6H_4-isoqui)}(H_2O)$_2$]X (X = BF_4 (**9a[BF$_4$]**), OTf (**9a[OTf]**)). Salt **9a[BF$_4$]** reacts with 2-(2-pinacolborylphenyl)-5-methylpyridine in the presence of 40 equiv of K_3PO_4 to afford Ir{κ^2-*C*,*C*-(C_6H_4-ImMe)}{κ^2-*C*,*N*-(C_6H_4-isoqui)}{κ^2-*C*,*N*-(C_6H_4-Mepy)} (**10a**). Complexes **6a**, **6b**, **7a**, **7b**, **8a**, **8b**, and **10a** are phosphorescent emitters (λ_{em} = 465–655 nm), which display short lifetimes in the range 0.2–5.6 μs. They show high quantum yields both in doped poly(methyl methacrylate) films (0.34–0.87) and in 2-methyltetrahydrofuran at room temperature (0.40–0.93). From the point of view of their applicability to the fabrication of OLED devices, a notable improvement with regard to those containing two cyclometalated *C*,*N*-ligands is achieved. The introduction of the cyclometalated aryl-NHC group allows reaching a brightness of 1000 cd/m^2 at a lower voltage and appears to give rise to higher luminous efficacy and power efficacy.

Introduction

The energy of the excited states in d^6 complexes is ligand dependent. As a consequence, the photophysical properties of phosphorescent emitters can be governed by selection of appropriate ligands to form the metal coordination sphere.[1] However, complexes containing different ligands on the metal center show a marked tendency to undergo ligand distribution processes, which involve dissociation and substitution reactions.[2] Iridium(III) is a $5d^6$ ion exhibiting a high octahedral Δ_0 splitting. Thus, the electron configuration of the metal center is always of low-spin and the ligand-field stabilization energy is maximized.[3] This means that octahedral iridium(III) complexes are significantly stable and rather inert toward substitution.[4] As a consequence, there is a growing interest in heteroleptic phosphorescent iridium(III) complexes,[5] which have been positioned at the forefront of modern photochemistry, since it seems to be possible to design stable species with bespoke excited-state properties according to the requirements of a given application.[6]

Ionic transition metal complexes have been employed in light-emitting electrochemical cells (LECs) as emitters,[7] in particular cyclometalated iridium(III) cations since they are readily accessible through the use of neutral *N*,*N*-chelate ligands derived from bipyridines.[8] However, neutral compounds are better emitters for organic light-emitting diode (OLED) technologies.[9] Thus, molecular iridium(III) derivatives stabilized by 2- or 3-electron donor bidentate ligands (2b or 3b) are arousing more interest than iridium(III) salts, specifically those containing at least two different ligands.[10]

Neutral iridium(III) complexes containing three different bidentate ligands are the most challenging. They are limited to some examples, which are based on two different orthometalated 2-phenylpyridines and a third ligand. The latter is usually acetylacetonate,[2,11]

although compounds of this type with 8-benzenesulfonamidoquinolinate and 1-(4-methylphenyl)isoquinolinate are also known.[12] Recently, orthometalated 2-phenylpyridine, or 2-(2,4-difluorophenyl)pyridine, has been combined with orthometalated phenylpyrazole or 1-(2,4-difluorophenyl)pyrazole and acetylacetonate,[13] whereas complexes bearing a neutral 4,4'-di-*t*-butyl-2,2'-bipyridine (4b), a monoanionic orthometalated 2-phenylpyridine (3b'), and a dianionic ligand, derived from 5,5'-di(trifluoromethyl)-3,3'-bipyrazole or 5,5'-(1-methylethylidene)-bis-(3-trifluoromethyl-1H-pyrazole) (2b"), form the novel type of [4b+3b'+2b"] emitters.[14]

N-Heterocyclic carbenes (NHCs) have the ability to tune the electron density of the metallic core.[15] As a consequence, they are powerful tools in several fields,[16] including material science.[17] Remarkable M-NHC π-backbonding has been found in complexes with electron rich metal centers, in particular for those based on third row metals.[18] Thus, the cyclometalated arylpyridines, widely used to prepare emitters for OLEDs, are being replaced by cyclometalated aryl-NHCs because of the latter effectively raise the LUMO energy, which gives rise to a wider band gap and therefore more energetic emissions.[19] In the search for an efficient tuning of the color and stable systems towards ligand redistribution issues, we decided to prepare tris-heteroleptic iridium(III) complexes in which one of the cyclometalated ligands is an aryl-NHC group.

This paper reports easy procedures to prepare phosphorescent heteroleptic iridium(III) emitters with three markedly different 3-electron donor chelate ligands, which are stable toward ligand redistribution processes and allow a color tuning in a wide range of emission wavelengths. Furthermore, we show that the replacement of a cyclometalated *C*,*N*-ligand (3b) in heteroleptic [3b+3b+3b'] iridium(III) complexes by a cyclometalated *C*,*C*-aryl-NHC group allows the fabrication of an OLED device with better electroluminescence performance.

Results and Discussion

Preparation of [Ir(μ-Cl)(3b)(3b')]$_2$ Dimers Containing a Cyclometalated Aryl-NHC Ligand. Iridium(III) emitters of type [3b+3b'+3b"] bearing two different cyclometalated aryl-N-heterocycles and a third ligand, generally acetylacetonate (acac), are prepared by means of an adaption of the standard synthesis of [3b+3b+3b'] complexes, based upon the formation of [Ir(μ-Cl)(3b)$_2$]$_2$ dimers. In this method, [Ir(μ-Cl)(COD)]$_2$ (**1**; COD = 1,5-cyclooctadiene) or $IrCl_3 \cdot 3H_2O$ are refluxed in 2-methoxyethanol or a mixture of the latter and water with two different cyclometalating aryl-N-heterocycles. The reactions lead to a complex mixture of [Ir(μ-Cl)(3b)$_2$]$_2$, [Ir(μ-Cl)(3b')$_2$]$_2$, and [Ir(μ-Cl)(3b)(3b')]$_2$ species. Then the mixture is directly treated with acetylacetone in basic 2-ethoxyethanol to afford a new mixture of Ir(3b)$_2$(acac), Ir(3b')$_2$(acac), and Ir(3b)(3b')(acac), which are separated by column cromatography.[2,11a-d] An alternative method that directly yields [Ir(μ-X)(3b)(3b')]$_2$ dimers involves the degradation of [3b+3b+3b'] complexes in the presence of Lewis acids containing a X halogen.[11e] Recently Aoki and co-workers have reported a novel procedure based upon ligand-selective electrophilic reactions, via interligand HOMO hopping phenomena.[12a]

The particularities of the NHC ligands make the application of the previously mentioned procedures unviable in our case. In view of this situation, we decided to prepare an Ir(I)-NHC species which would promote both NHC- and pyridyl-supported C-H bond activations of the corresponding aryl substituents,[20] to generate the [Ir(μ-Cl)(3b)(3b')]$_2$ synthetic key intermediates. In order to develop the procedure to obtain our target compounds, we selected 1-phenyl-3-methylimidazolylidene (PhMeIm) as model of NHC ligand and the dimer [Ir(μ-Cl)(COD)]$_2$ (**1**) as starting point. The NHC ligand was introduced into the iridium coordination sphere by transmetalation from the silver species PhMeImAgI, which was generated *in situ* by the

procedure previously described by Rourke and co-workers[21] and used by Wang and co-workers,[22] Crabtree and co-workers,[23] and us[24] to prepare platinum(II), iridium(I), and osmium(II) derivatives, respectively. The transmetalation affords the square-planar mononuclear compound IrCl(COD)(PhMeIm) (**2**), which was isolated as a yellow solid in 92% (Scheme 1). In agreement with the presence of a coordinated NHC ligand, the $^{13}C\{^{1}H\}$ NMR spectrum of the obtained solid, in dichloromethane-d_2, at room temperature shows a singlet at 181.2 ppm due to the metalated carbon atom of the imidazolylidene group. In addition, four singlets at 83.9, 83.6, 52.1 and 51.9 ppm, corresponding to the olefinic C(sp^2) atoms should be mentioned. These signals, along with olefinic C-H resonances at 4.58, 4.40, 2.89, and 2.24 ppm in the ^{1}H NMR spectrum, indicate a restricted rotation of the NHC ligand around the Ir-NHC bond.

Scheme 1. Synthesis of Complex IrCl(COD)(PhMeIm) (2)

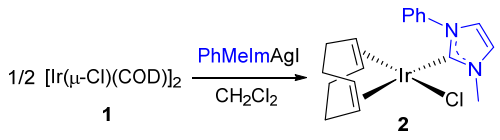

Complex **2** reacts with 1-phenylisoquinoline, 2-phenylpyridine, and 2-(2,4-difluorophenyl)pyridine in methanol under reflux to give after 3-5 days the desired dimers [Ir(μ-Cl){κ^2-*C,C*-(C_6H_4-ImMe)}{κ^2-*C,N*-(C_6H_4-isoqui)}]$_2$ (**3**), [Ir(μ-Cl){κ^2-*C,C*-(C_6H_4-ImMe)}{κ^2-*C,N*-(C_6H_4-py)}]$_2$ (**4**), and [Ir(μ-Cl){κ^2-*C,C*-(C_6H_4-ImMe)}{κ^2-*C,N*-($C_6F_2H_2$-py)}]$_2$ (**5**), as a result of the NHC- and pyridyl- directed *ortho*-CH bond activation of the aryl substituents of the coordinated imidazolylidene group and the added heterocycle and the hydrogenation of a C-C double bond of the coordinated diene, which is released. These dimers were isolated as orange (**3**) and pale yellow (**4** and **5**) solids in high yield (70-81%) (Scheme 2).

Scheme 2. Synthesis of Dimers 3, 4, and 5

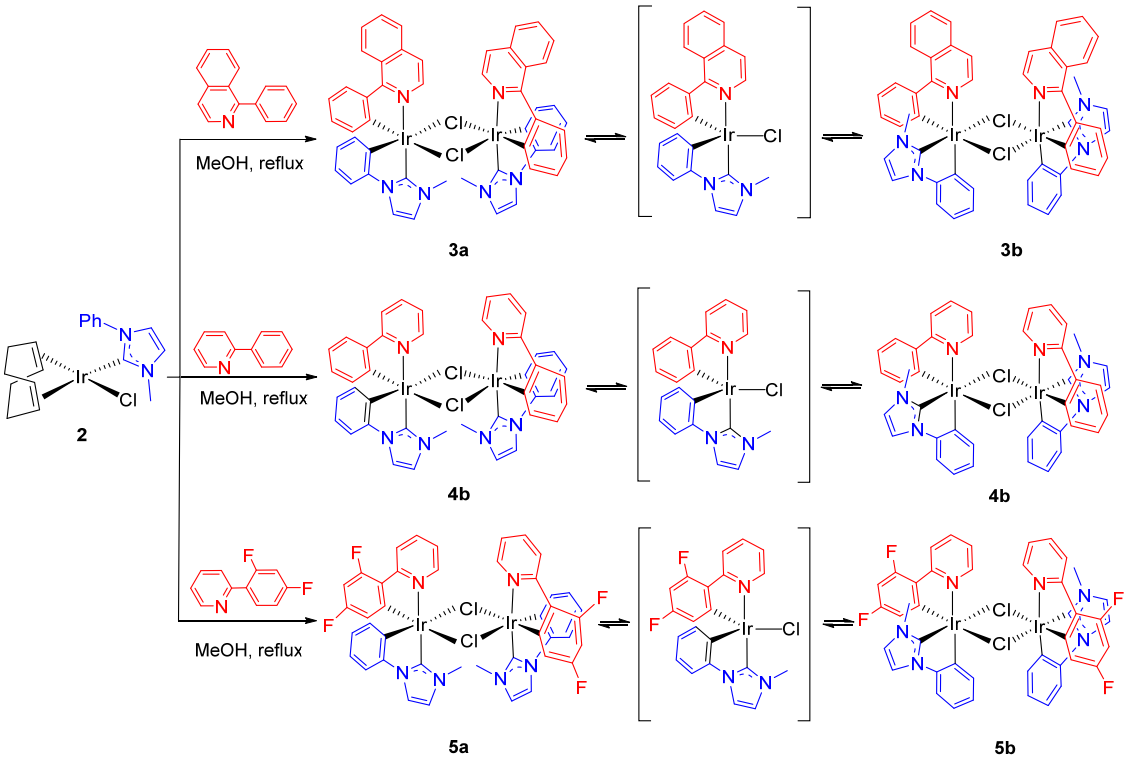

The $^{13}C\{^{1}H\}$ and ^{1}H NMR spectra of the obtained solids, in dichloromethane-d_2, at room temperature reveal that they exist as a mixture of isomers **a** (Im *trans* to N) and **b** (Im *trans* to Cl), which lie in a dynamic equilibrium. Figure 1 shows the $^{1}H,^{1}H$ 2D NOESY spectrum of **3**. This type of spectra contains cross peaks from both NOE interactions and peaks due to isomers in slow exchange with one another on the NMR time scale. The NOE cross peaks are of opposite sign compared to the diagonal peaks. However, the cross peaks resulting from the slow exchanging isomers are of the same sign as the diagonal peaks. In agreement with a slow isomerization process between **a** and **b**, this spectrum contains cross peaks of the same sign as the diagonal peaks (orange peaks), which are ostensible in the region at about 9.3 ppm and between 3.9 and 3.1 ppm. The isomerization could take place via five-coordinate mononuclear IrCl(3b)(3b') intermediates, resulting from the rupture of the chloride bridges. In addition, it

should be pointed out that homoleptic dimers are not observed, in contrast to the systems bearing two different arylpyridines.

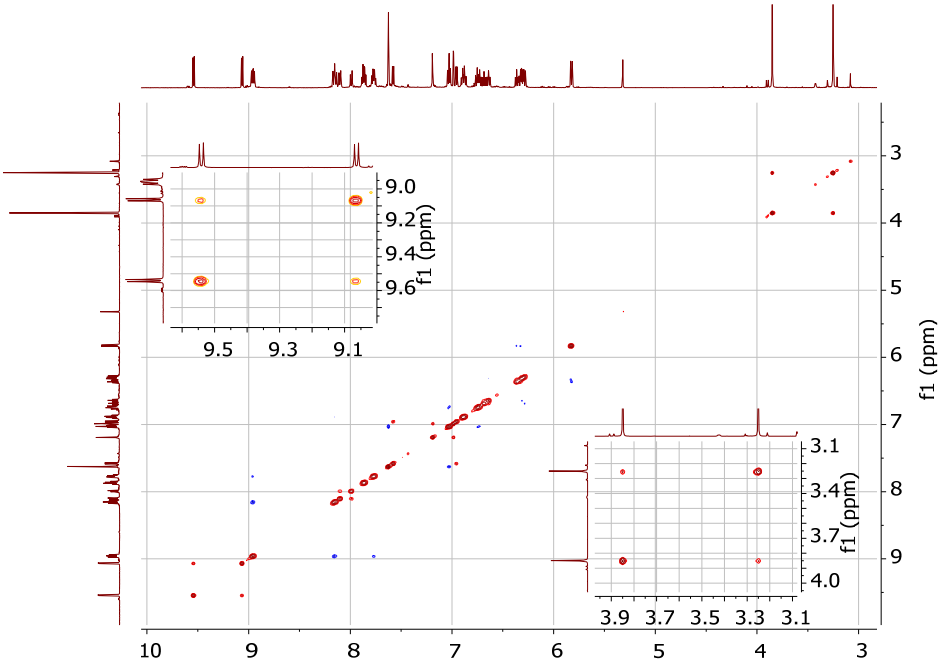

Figure 1. $^{1}H,^{1}H$ 2D NOESY spectrum of **3** (500 MHz, CD_2Cl_2, d8 = 1 s).

Crystals of **3a** suitable for X-ray diffraction analysis were obtained from the mixture of isomers. The structure (Figure 2) demonstrates the efficiency of the procedure to prepare [Ir(μ-Cl)(3b)(3b')]$_2$ dimers with cyclometalated aryl-NHC and aryl-N-heterocycle ligands. The coordination polyhedron around each iridium atom can be described as a distorted octahedron with the imidazolylidene and isoquinolyl groups disposed mutually *trans* (N(1)-Ir(1)-C(16) = 171.0(3)^{o} and N(4)-Ir(2)-C(41) = 167.8(3)^{o}). At the perpendicular plane, the metalated carbon atoms of the phenyl substituents are situated *trans* to the bridging chlorides (C(11)-Ir(1)-Cl(2) = 172.5(3)^{o}, C(21)-Ir(1)-Cl(1) = 173.2(3)^{o}, C(36)-Ir(2)-Cl(1) = 172.3(2)^{o}, and C(46)-Ir(2)-Cl(2) = 172.6(3)^{o}). The Ir-imidazolylidene bond lengths of 1.979(10) (Ir(1)-C(16)) and 1.990(10) (Ir(2)-C(41)) Å are consistent with normal Ir-NHC bonds,[25] whereas the Ir-aryl distances of 1.975(10)

(Ir(1)-C(11), 1.992(10) (Ir(1)-C(21)), 1.967(9) (Ir(2)-C(36)), and 2.013(10) (Ir(2)-C(46)) Å compare well with those reported for related five-membered iridacycles.[5c,26]

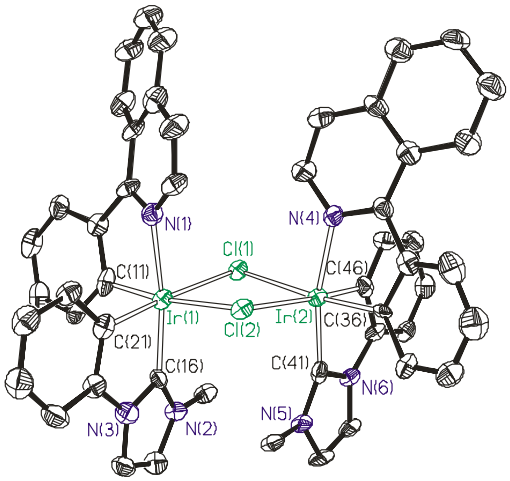

Figure 2. Molecular diagram of complex **3a** (50% probability ellipsoids). Hydrogen atoms are omitted for clarity. Selected bond lengths (Å) and angles (deg): Ir(1)-Cl(1) = 2.497(2), Ir(1)-Cl(2) = 2.519(2), Ir(1)-N(1) = 2.101(8), Ir(1)-C(21) = 1.992(10), Ir(1)-C(11) = 1.975(10), Ir(1)-C(16) = 1.979(10), Ir(2)-Cl(1) = 2.510(2), Ir(2)-Cl(2) = 2.518(2), Ir(2)-N(4) = 2.092(8), Ir(2)-C(36) = 1.967(9), Ir(2)-C(46) = 2.013(10), Ir(2)-C(41) = 1.990(10); N(1)-Ir(1)-C(16) = 171.0(3), C(21)-Ir(1)-Cl(1) = 173.2(3), C(11)-Ir(1)-Cl(2) = 172.5(3), N(4)-Ir(2)-C(41) = 167.8(3), C(36)-Ir(2)-Cl(1) = 172.3(2), C(46)-Ir(2)-Cl(2) = 172.6(3).

Formation of [3b+3b'+3b'']-Aryl-NHC Complexes with an Acetylacetonate Ligand. Mixtures **3**, **4**, and **5** react with Kacac to give the corresponding acetylacetonate derivatives, as a result of the rupture of the bridges and the replacement of the chloride ligands by an acac group (Scheme 3). Thus, the treatment of **3a** and **3b**, **4a** and **4b**, and **5a** and **5b** with the salt in tetrahydrofuran, at 60°C, for 90 min leads to mixtures of isomers **a** (Im *trans* to N) and **b** (Im *trans* to O) of Ir{κ^2-*C*,*C*-(C_6H_4-ImMe)}{κ^2-*C*,*N*-(C_6H_4-isoqui)}(κ^2-*O*,*O*-acac) (**6**), Ir{κ^2-*C*,*C*-(C_6H_4-ImMe)}{κ^2-*C*,*N*-(C_6H_4-py)}(κ^2-*O*,*O*-acac) (**7**), and Ir{κ^2-*C*,*C*-(C_6H_4-ImMe)}{κ^2-*C*,*N*-

($C_6F_2H_2$-py)}(κ^2-*O*,*O*-acac) (**8**). The isomers were separated by column chromatography and were obtained as pure red (**6a**), orange (**6b**), or yellow (**7a**, **7b**, **8a** and **8b**) solids in 24% (**6a**), 11% (**6b**), 43 % (**7a**), 21% (**7b**), 60% (**8a**), and 10% (**8b**) yield. When the reaction of **3** with Kacac was performed in tetrahydrofuran:methanol 2:1, complex **6a** was exclusively obtained in 66% yield after the crude purification by column chromatography. The stereochemistries were confirmed by means of the X-ray diffraction analysis of **6a**, **7a**, and **7b**.

Scheme 3. Synthesis of Mononuclear Complexes 6a, 6b, 7a, 7b, 8a, and 8b

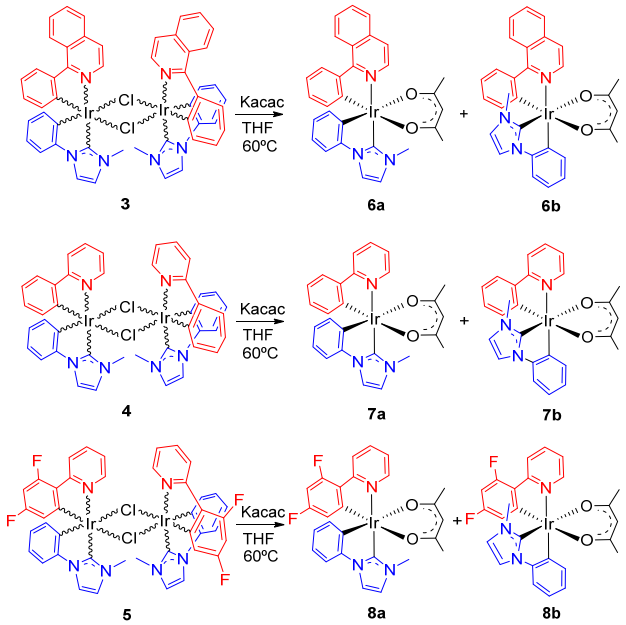

Figure 3 shows a view of **6a**. The coordination geometry around the iridium atom can be rationalized as a distorted octahedron with the imidazolylidene and isoquinolyl groups mutually *trans* disposed (C(1)-Ir-N(3) = 170.68(11)º). The donor atoms of the cyclometalated phenyl substituents lie at the perpendicular plane, disposed *trans* to the oxygen atoms of the acac group, with C(6)-Ir-O(2) and C(21)-Ir-O(1) angles of 178.48(9)º and 172.24(10)º, respectively. The Ir-imidazolylidene bond length of 1.982(3) (Ir-C(1)) Å and the Ir-aryl distances of 2.013(3) (Ir-C(6)) and 1.985(3) (Ir-C(21)) Å compare well with those of **3a**. The most noticeable

spectroscopic feature of **6a** is the chemical shift (δ, 165.4) of the resonance due to the metalated carbon C(1) of the imidazolylidene group in the $^{13}C\{^{1}H\}$ NMR spectrum, in dichloromethane-d_2, at room temperature, which appears shifted by 10.8 ppm towards lower field with regard to that of isomer **6b**. The latter is observed at 154.6 ppm.

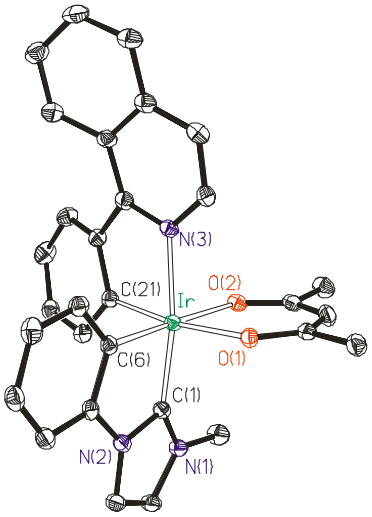

Figure 3. Molecular diagram of complex **6a** (50% probability ellipsoids). Hydrogen atoms are omitted for clarity. Selected bond lengths (Å) and angles (deg): Ir-O(1) = 2.155(2), Ir-O(2) = 2.149(2), Ir-N(3) = 2.101(2), Ir-C(1) = 1.982(3), Ir-C(6) = 2.013(3), Ir-C(21) = 1.985(3); N(3)-Ir-C(1) = 170.68(11), O(1)-Ir-C(21) = 172.24(10), O(2)-Ir-C(6) = 178.48(9), C(1)-Ir-C(6) = 79.49(12), C(21)-Ir-N(3) = 79.83(11), O(1)-Ir-O(2) = 87.82(8).

Figure 4 shows a view of **7a**. The geometry of the metal center resembles that of **6a**, with a cyclometalated 2-phenylpyridine ligand occupying the positions of the cyclometalated 1-phenylisoquinoline group, a imidazolylidene-Ir-pyridyl angle C(1)-Ir-N(3) of 172.57(18)°, aryl-Ir-acac angles C(6)-Ir-O(2) and C(11)-Ir-O(1) of 178.61(16)° and 171.23(17)°, respectively, and Ir-Im and Ir-aryl bond lengths of 1.990(5) (Ir-C(1)), 2.018(5) (Ir-C(6)), and 1.989(5) (Ir-C(11)) Å. In agreement with **6a**, the $^{13}C\{^{1}H\}$ NMR spectrum of **7a**, in dichloromethane-d_2, at room temperature shows a singlet at 164.8 ppm due to the atom C(1) of the imidazolylidene group.

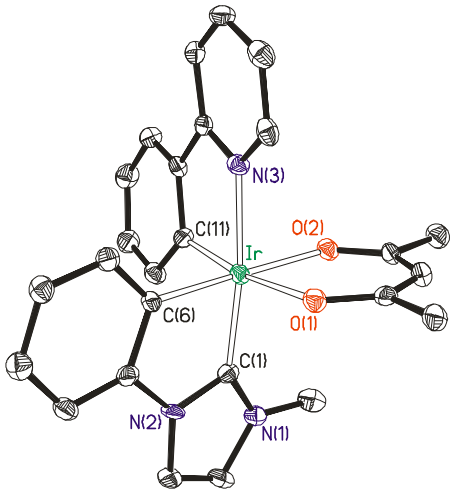

Figure 4. Molecular diagram of complex **7a** (50% probability ellipsoids). Hydrogen atoms are omitted for clarity. Selected bond lengths (Å) and angles (deg): Ir-O(1) = 2.155(3), Ir-O(2) = 2.139(3), Ir-N(3) = 2.097(4), Ir-C(1) = 1.990(5), Ir-C(6) = 2.018(5), Ir-C(11) = 1.989(5); N(3)-Ir-C(1) = 172.57(18), O(1)-Ir-C(11) = 171.23(17), O(2)-Ir-C(6) = 178.61(16), C(1)-Ir-C(6) = 79.7(2), C(11)-Ir-N(3) = 80.40(19), O(1)-Ir-O(2) = 88.18(13).

Figure 5 shows a view of **7b**. The geometry around the metal center resembles that of **7a**, changing the disposition of the *C*,*C*-chelate ligand; i.e., the metalated phenyl group is now disposed trans to the nitrogen atom of the heterocycle (C(6)-Ir-N(3) = 176.4(3)º), while the imidazolylidene lies trans to the O(1) atom of the acetylacetonate ligand (C(1)-Ir-O(1) = 174.0(3)º). The other oxygen atom is located trans to the phenyl substituent of the pyridine with a C(11)-Ir-O(2) angle of 173.6(3)º. The Ir-imidazolylidene bond length of 1.938(10) (Ir-C(1)) Å and the Ir-aryl distances of 2.074(9) (Ir-C(6)) and 1.991(9) (Ir-C(11)) Å display values similar to those of **7a**. Like in **6**, the change in the disposition of the imidazolylidene group produces a 10.8 ppm higher field shift of the C(1) resonance (δ, 154.0) in the $^{13}C\{^{1}H\}$ NMR spectrum.

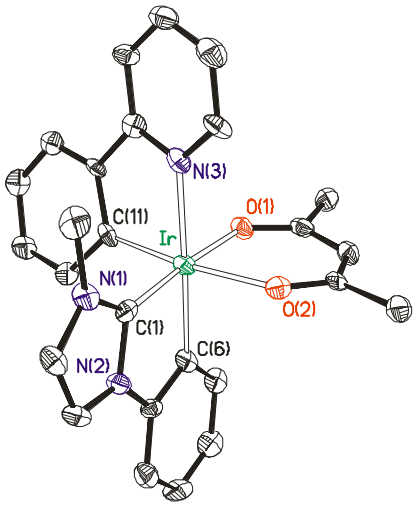

Figure 5. Molecular diagram of complex **7b** (50% probability ellipsoids). Hydrogen atoms are omitted for clarity. Selected bond lengths (Å) and angles (deg): Ir-O(1) = 2.114(6), Ir-O(2) = 2.167(6), Ir-N(3) = 2.125(8), Ir-C(1) = 1.938(10), Ir-C(6) = 2.074(9), Ir-C(11) = 1.991(9); N(3)-Ir-C(6) = 176.4(3), O(1)-Ir-C(1) = 174.0(3), C(11)-Ir-O(2) = 173.6(3), C(1)-Ir-C(6) = 79.4(4), C(11)-Ir-N(3) = 79.4(3), O(1)-Ir-O(2) = 88.8(2).

The comparison of the $^{13}C\{^{1}H\}$ NMR spectra of **8a** and **8b** reveals the same trend as that found in the isomers **a** and **b** of **6** and **7**. In the $^{13}C\{^{1}H\}$ NMR spectrum of **8a**, the resonance corresponding to the metalated carbon atom of the imidazolylidene group is observed at 163.8 ppm, shifted 10.9 ppm to lower field with regard to that of **8b**, which appears at 152.9 ppm.

Replacement of the Acetylacetonate Ligand of 6a by a Cyclometalated 2-Phenyl-5-methylpyridine. Gray and co-workers have recently reported the preparation of cyclometalated iridium(III) complexes by base-assisted transmetalation reactions starting from *cis*-bis(aquo) iridium compounds and boronated aromatic proligands.[27] Because the procedure afforded high yields, we decided to adapt it to our needs (Scheme 4).

Scheme 4. Synthesis of [3b+3b'+3b''] Complexes 10a and 10 a'

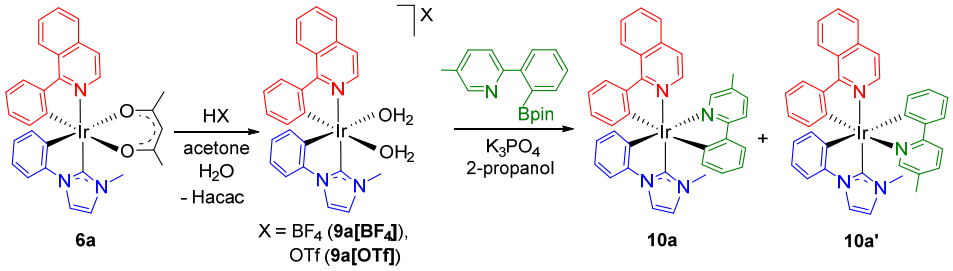

Treatment of 3.1:1 acetone:water solutions of **6a** with 7 equiv of tetrafluoroboric acid ($HBF_4{\cdot}OEt_2$) or triflic acid (HOTf), at room temperature for 24 h produces the protonation of the acetylacetonate ligand, which is replaced by water molecules to afford the bis(aquo) cation $[Ir\{\kappa^2\text{-}C,C\text{-}(C_6H_4\text{-ImMe})\}\{\kappa^2\text{-}C,N\text{-}(C_6H_4\text{-isoqui})\}(H_2O)_2]^+$ (**9a**). Its BF_4- and OTf-salts (**9a[BF4]** and **9a[OTF]**, respectively) were isolated as red solids in ca. 65% yield. Figure 6 shows a view of the cation of **9a[OTF]**. The geometry around the iridium atom resembles that of the starting compound with the water molecules in the positions of the acac-oxygen atoms, and an imidazolylidene-Ir-isoquinolyl angle C(1)-Ir-N(1) of 171.5(2)º, aryl-Ir-water angles C(6)-Ir-O(1) and C(11)-Ir-O(2) of 175.11(19)º and 170.4(2)º, and Ir-Im and Ir-aryl distances of 1.992(6) (Ir-C(1)) and 2.012(6) (Ir-C(6)) and 1.986(6) (Ir-C(11)) Å. In agreement with the presence of the coordinated water molecules in the cation, its ^1H NMR spectrum, in dichloromethane-d_2, at room temperature shows the characteristic H_2O resonance centered at 4.30 ppm. In the $^{13}C\{^1H\}$ NMR spectrum, the most noticeable feature is the resonance corresponding to the imidazolylidene C(1) carbon atom, which appears at 161.8 ppm.

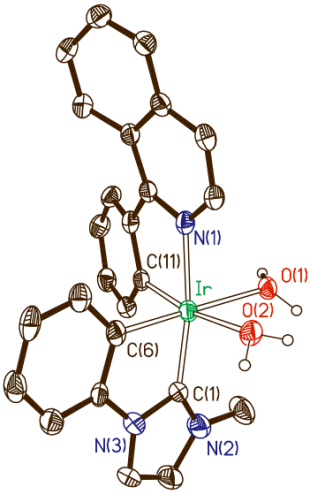

Figure 6. Molecular diagram of the cation of **9a[OTf]** (50% probability ellipsoids). Most hydrogen atoms are omitted for clarity. Selected bond lengths (Å) and angles (deg): Ir-O(1) = 2.216(4), Ir-O(2) = 2.224(4), Ir-N(1) = 2.095(5), Ir-C(1) = 1.992(6), Ir-C(6) = 2.012(6), Ir-C(11) = 1.986(6); N(1)-Ir-C(1) = 171.5(2), O(1)-Ir-C(6) = 175.11(19), O(2)-Ir-C(11) = 170.4(2), C(1)-Ir-C(6) = 80.0(2), C(11)-Ir-N(1) = 80.1(2), O(1)-Ir-O(2) = 83.66(15).

Pinacolboryl efficiently transfers cyclometalating *N*,*C*-ligands to the [Ir{κ^2-*C*,*C*-(C_6H_4-ImMe)}{κ^2-*C*,*N*-(C_6H_4-isoqui)}]$^+$ metal fragment in agreement with the observations of Gray and co-workers. However, the reactions are more complex in our case, due to the asymmetry of both the receptor fragment and the proligand, which can give rise to mixtures of stereoisomers. Thus, the treatment of 2-propanol solutions of **9a[BF_4]** with 2-(2-pinacolborylphenyl)-5-methylpyridine in the presence of K_3PO_4, for 24 h, at room temperature leads to mixtures of the isomers **10a** and **10a'** of the tris-heteroleptic iridium(III) complex Ir{κ^2-*C*,*C*-(C_6H_4-ImMe)}{κ^2-*C*,*N*-(C_6H_4-isoqui)}{κ^2-*C*,*N*-(C_6H_4-Mepy)} (**10**), containing two different cyclometalated aryl-N-heterocycles and a cyclometalated aryl-NHC (Figures 7 and 8). The molar ratio between the isomers is independent of the used boronated precursor:iridium molar ratio, in the range from 1 to 15 (Figure 7). However, the amount of isomer **10a** increases with the amount of K_3PO_4 added

to the reaction. Its formation becomes exclusive when K_3PO_4:iridium molar ratios higher than 40 are used (Figure 8).

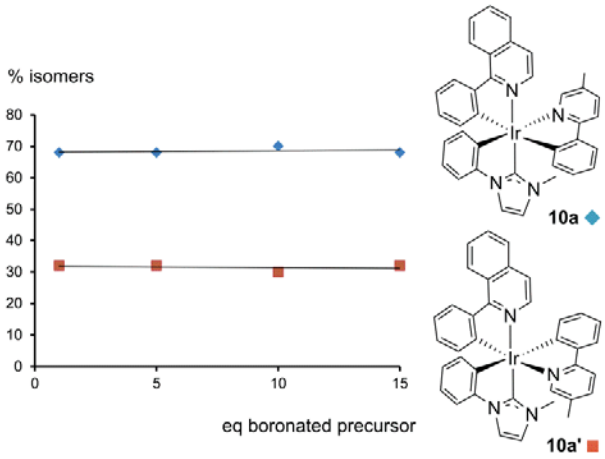

Figure 7. Ratio of isomers **10a**:**10a'** as a function of the amount of boronated precursor used (experiments performed in a ratio **9a[BF_4]**:K_3PO_4 of 1:5).

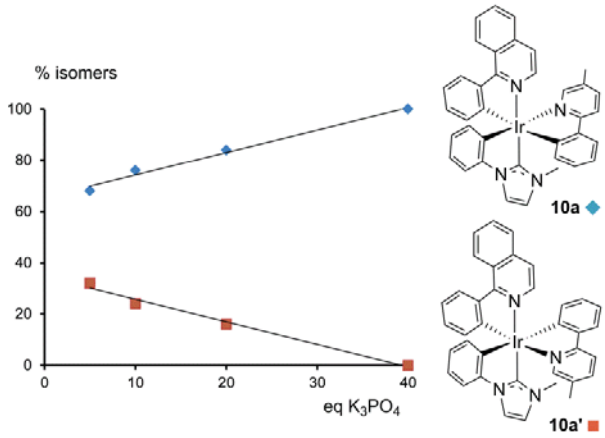

Figure 8. Ratio of isomers **10a**:**10a'** as a function of the equivalents of K_3PO_4 used (experiments performed in a ratio **9a[BF_4]**:boronated precursor of 1:1).

Isomer **10a** was isolated as a red solid in 66% yield and characterized by X-ray diffraction analysis. The structure has two chemically equivalent but crystallographically independent molecules in the asymmetric unit. Figure 9 shows one of them. Noticeable features of its octahedral environment are the stereochemistry of the Ir{κ^2-*C*,*C*-(C_6H_4-ImMe)}{κ^2-*C*,*N*-(C_6H_4-

isoqui)} skeleton, which is retained with regard to **3a** and **6a** (N(1)-Ir(1)-C(28) = 171.42(19)º and 170.86(19)º), and the disposition *trans* of the pyridyl group and the metalated aryl substituent of the NHC ligand (N(2)-Ir(1)-C(33) = 171.33(18)º and 174.35(18)º). The aryl substituents of the heterocycles, which are also disposed mutually *trans*, form aryl-Ir-aryl angles of 174.0(2)º and 172.1(2)º (C(1)-Ir(1)-C(16)). In the $^{13}C\{^{1}H\}$ NMR spectrum, in dichloromethane-d_2, at room temperature, the resonance due to the metalated C(28) atom of the imidazolylidene moiety appears at 164.5 ppm, whereas that corresponding to the analogous atom of **10a'** is observed at 166.7 ppm.

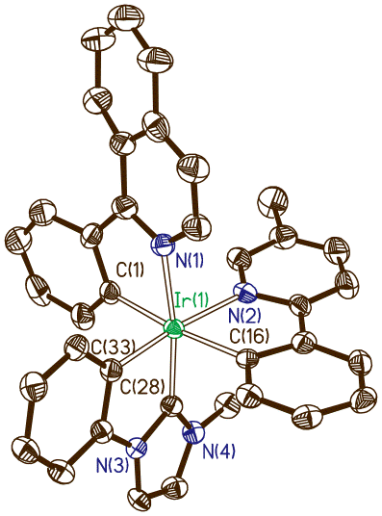

Figure 9. Molecular diagram of one of the two independent molecules of complex **10a** in the asymmetric unit (50% probability ellipsoids). Hydrogen atoms are omitted for clarity. Selected bond lengths (Å) and angles (deg): Ir(1)-N(1) = 2.097(4), 2.101(4), Ir(1)-N(2) = 2.133(4), 2.135(4), Ir(1)-C(1) = 2.052(5), 2.050(5), Ir(1)-C(16) = 2.087(5), 2.071(5), Ir(1)-C(28) = 1.980(5), 1.976(5), Ir(1)-C(33) = 2.029(5), 2.033(5); N(1)-Ir(1)-C(28) = 171.42(19), 170.86(19), N(2)-Ir(1)-C(33) = 171.33(18), 174.35(18), C(1)-Ir(1)-C(16) = 174.0(2), 172.1(2), C(1)-Ir(1)-N(1) = 78.7(2), 78.31(19), C(16)-Ir(1)-N(2) = 78.40(18), 77.7(2), C(28)-Ir(1)-C(33) = 79.8(2), 79.7(2).

Photophysical Properties of the [3b+3b'+3b'']-Aryl-NHC Complexes. The UV/vis absorption data of 2-methyltetrahydrofuran (2-MeTHF) solutions of isomers **a** and **b** of **6**–**8** and **10a**, at room temperature, are collected in Table 1. The spectra show bands in three different zones of energy: <320, 320–500, and >500 nm for **6a**, **6b**, and **10a** and <320, 320–450, and >450 nm for **7a**, **7b**, **8a**, and **8b**. Time dependent DFT calculations (B3LYP-GD3//SDD(f)/6-31G**), computed in tetrahydrofuran as solvent, indicate that the absorptions of the highest energy region correspond to $^{1}\pi$-π* interligand transitions, mainly from the *C*,*C*-group to the *C*,*N*-ligands. For the phenylisoquinolinate complexes **6a**, **6b**, and **10a**, the bands in the region of moderate energy are due to allowed spin metal-to-phenylisoquinolinate charge transfer (^{1}MLCT) mixed with *C*,*C*-ligand-to-phenylisoquinolinate and acac-to-phenylisoquinolinate transitions for **6a** and **6b**. For complexes **7a**, **7b**, **8a**, and **8b**, the bands in the region of moderate energy are due to allowed spin metal-to-*C*,*N*-ligand charge transfer (^{1}MLCT) mixed with *C*,*C*-ligand- and acac-to-*C*,*N*-ligand transitions. The weak absorptions tails after 500 nm for **6a**, **6b**, and **10a** or after 450 nm for **7a**, **7b**, **8a**, and **8b** are usually assigned to formally spin-forbidden ^{3}MLCT transitions caused for the large spin-orbit coupling introduced by the iridium center.[2,5e,11-14]

The electrochemical properties of isomers **6a**, **7a**, **8a**, and **10a** were studied using cyclic voltammetry in degassed acetonitrile solutions and referenced versus Fc/Fc^{+}. The results are summarized in Table 2. All complexes showed a reversible one-electron oxidation process between 0.17 and 0.51 V. For the phenylisoquinolinate derivatives **6a** and **10a**, quasireversible reduction waves at -2.25 and -2.28 V, respectively, were also observed, whereas no obvious reduction peaks were observed for **7a** and **8a** within the solvent window. The observed

Table 1. Selected Experimental UV-vis Absorption Data for 6–8 and 10a (in 2-MeTHF) and Computed TD-DFT (in THF) Vertical Excitation Energies and Their Major Contributions

complex	λ_{exp} (nm)	ε ($M^{-1}cm^{-1}$)	excitation energy (nm)	Oscillator strength *f*	transition	contrib (%)
6a	240	34000	245	0.0848	HOMO-3→LUMO+4	54
	348	4500	355	0.1235	HOMO-3→LUMO	94
	488	600	501	0.0446	HOMO→LUMO	98
	524	300				
6b	242	60500	242	0.1004	HOMO-5→LUMO+3	20
					HOMO-4→LUMO+3	19
	350	14500	329	0.1774	HOMO-4→LUMO	47
	470	2500	497	0.0717	HOMO→LUMO	96
	534	600				
7a	240	40100	269	0.1206	HOMO-7→LUMO	51
	338	5100	338	0.0575	HOMO-2→LUMO	85
	450	1200	425	0.0335	HOMO→LUMO	97
	484	200				
7b	242	48300	246	0.0521	HOMO-2→LUMO+4	57
	342	7500	343	0.0728	HOMO-2→LUMO	90
	430	1200	416	0.0313	HOMO→LUMO	97
	452	500				
8a	242	29600	263	0.1331	HOMO-3→LUMO+2	65
	334	3000	334	0.0611	HOMO-2→LUMO	78
	415	300	412	0.0289	HOMO→LUMO	96
	440	200				
8b	248	28900	304	0.0615	HOMO-3→LUMO	81
	330	7900	336	0.0154	HOMO→LUMO+2	93
	426	1400	406	0.0255	HOMO→LUMO	97
	452	500				
10a	237	44500	255	0.1113	HOMO-1→LUMO+8	47
	282	30000	277	0.1369	HOMO-3→LUMO+3	55
	358	9800	338	0.0993	HOMO-5→LUMO	83
	502	1900	502	0.0321	HOMO→LUMO	98
	552	900				

electrochemical gap for **6a** and **10a** as well as the absence of observable reduction for **7a** and **8a** are in agreement with the computed HOMO-LUMO gap (Table 2, Tables S15–S21, and Figures S36–S42).

Table 2. Electrochemical and DFT MO Energy Data for Complexes 6a–8a and 10a

complex	$E_{1/2}^{ox}$[a] (V)	$E_{1/2}^{red}$[a] (V)	$E_{1/2}^{ox} - E_{1/2}^{red}$ (V)	HOMO[b] (eV)	LUMO[b] (eV)	HLG[b,c] (eV)
6a	0.34	-2.25	2.59	-4.90	-1.74	3.16
7a	0.36			-4.89	-1.23	3.66
8a	0.51			-5.05	-1.30	3.75
10a	0.17	-2.28	2.45	-4.84	-1.69	3.15

[a]Measured in degassed acetonitrile solution (1×10^{-3} M)/$[Bu_4N]PF_6$ (0.1 M), vs Fc/Fc^+ at 0.1 $V \cdot s^{-1}$, at room temperature. [b]Values from electronic structure DFT calculations. [c]HLG = LUMO – HOMO.

These [3b+3b'+3b'']-aryl-NHC derivatives are phosphorescent emitters upon photoexcitation, in doped poly(methyl methacrylate) (PMMA) film at 5 wt % and in powder, at room temperature, and in 2-methyltetrahydrofuran at room temperature and at 77 K. The phenylisoquinolinate complexes **6a**, **6b**, and **10a** emit in the red, displaying bands centered between 580 and 655 nm, whereas the emissions of compounds **7a**, **7b**, **8a**, and **8b** take place in the green between 465 and 532 nm. This difference in behavior is consistent with the HOMO-LUMO gaps shown in Table 2, which are higher for **7a** and **8a** than for the phenylisoquinolinate derivatives **6a** and **10a**. Figure 10 depicts the emission spectra in PMMA film (a), in 2-MeTHF at room temperature (b), and in 2-MeTHF at 77 K (c). Table 3 summarizes calculated and experimental wavelengths, lifetimes, quantum yields, and radiative and nonradiative rate constants. The emission spectra in PMMA film, in neat solid powder, and in 2-MeTHF at room temperature show broad structureless bands, while in 2-MeTHF at 77 K display vibronic fine

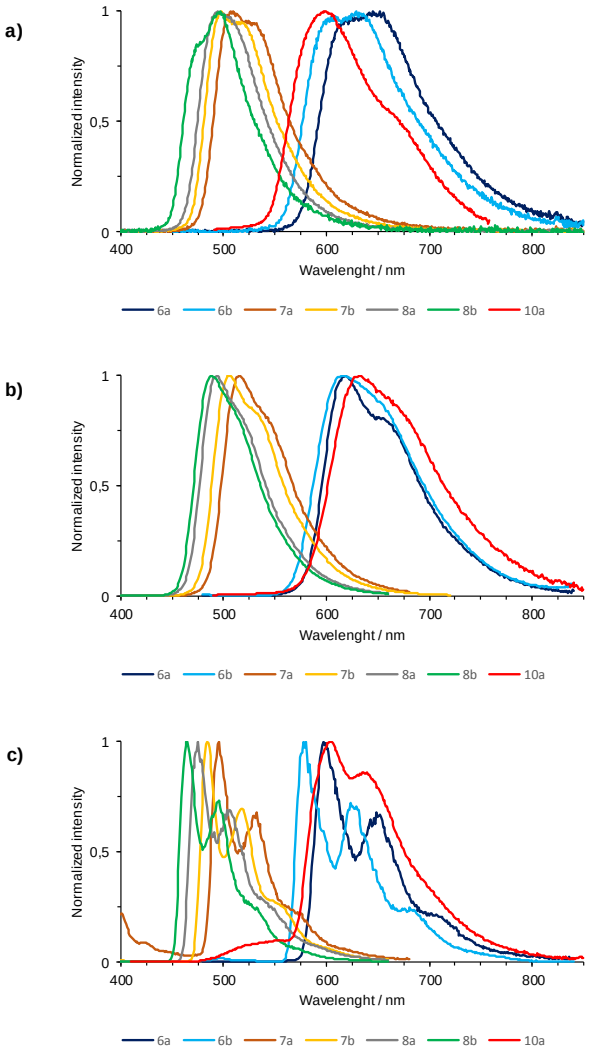

Figure 10. Emission spectra of complexes **6a–8b** and **10a** recorded in 5 wt % PMMA films at 298 K (a), in 2-MeTHF at 298 K (b), and in 2-MeTHF at 77K (c).

structures in a consistent manner with a significant contribution of ligand-centered $^3\pi$-π^* transitions to the excited state.[19d,28] The change in the orientation of the *C*,*C*-ligand produces a very modest shift of the emission wavelength. Thus, the emissions of isomers **b** appear slightly shifted toward the blue with regard to those of the respective isomers **a**. The introduction of the two fluoride substituents in the cyclometalated 2-phenylpyridine also gives rise to a moderated blue shift in the emissions. The lifetimes are short, lying in the range 0.2–5.6 μs. The quantum

yields were measured in doped PMMA film at 5 wt % and in 2-MeTHF solution. In PMMA film, the values are between 0.87 and 0.70 for the acac complexes **6**–**8** whereas for **10a**, where the acac ligand has been replaced by the cyclometalated 2-phenyl-5-methylpyridine, it decreases to 0.34. The same trend is observed in 2-MeTHF. The quantum yields for the acac derivatives lie between 0.93 and 0.56 whereas that of **10a** is 0.40. The radiative and nonradiative rate constants are in most cases of the same order of magnitude and similar in PMMA film and in solution.

The replacement of a *C*,*N*-ligand by a cyclometalated aryl-NHC group does not produce a significant shift of the emission. However, it increases significantly the quantum yield. For instance, the bis(phenylisoquinolinate) complex Ir{κ^2-*C*,*N*-(C_6H_4-isoqui)}$_2$(κ^2-*O*,*O*-acac) emits at 622 nm in dichloromethane with a quantum yield of 0.2,[29] which is about 4 times lower than those of **6a** and **6b**; the pyridyl derivative Ir{κ^2-*C*,*N*-(C_6H_4-py)}$_2$(κ^2-*O*,*O*-acac), which emits at 516 nm in 2-MeTHF with a quantum yield of 0.34,[30] is between twice and three times less efficient than **7a** and **7b**; and the fluoride disubstituted compound Ir{κ^2-*C*,*N*-($C_6F_2H_4$-py)}$_2$(κ^2-*O*,*O*-acac) displays an emission band at 482 nm in dichloromethane and shows a quantum yield of 0.63,[2,13] which is about 10% lower than those of **8a** and **8b**.

The emissions can be attributed to T_1 excited states originated by HOMO→LUMO charge transfer transitions. Figure 11 shows the spin density distribution calculated for the T_1 states at their minimum energy geometries. According to this, good agreement is observed between the experimental emissions and the calculated by estimating the difference in energy between the optimized triplet states and the singlet states S_0 in tetrahydrofuran.

Table 3. Photophysical Data for Complexes 6a, 6b, 7a, 7b, 8a, 8b and 10a

complex	calc λ_{em}[a] (nm)	media (T, K)	λ_{em} (nm)	λ_{exc} (nm)	τ (μs)	ϕ	k_r[b] (s^{-1})	k_{nr}[b] (s^{-1})	k_r/k_{nr}
6a		PMMA (298)	652	480	1.3	0.70	5.4×10^5	2.3×10^5	2.3
		powder (298)	655	590	1.0				
	638	2-MeTHF (298)	619	480	1.8	0.93	5.2×10^5	3.9×10^4	13.3
		2-MeTHF (77)	597, 652	420, 480	3.3				
6b		PMMA (298)	629	480	1.3	0.71	5.5×10^5	2.2×10^5	2.5
		powder (298)	629	570	0.9				
	633	2-MeTHF (298)	618	480	1.8	0.78	4.3×10^5	1.2×10^5	3
		2-MeTHF (77)	580, 623	415, 475	3.3				
7a		PMMA (298)	510	450	1.5	0.86	5.7×10^5	9.3×10^4	6.1
		powder (298)	526	490	0.4				
	516	2-MeTHF (298)	516	445	1.4	0.67	4.8×10^5	2.4×10^5	2.0
		2-MeTHF (77)	495, 532	455	5.0				
7b		PMMA (298)	498	455	1.3	0.77	5.9×10^5	1.8×10^5	3.3
		powder (298)	524	485	0.7				
	502	2-MeTHF (298)	505	445	1.1	0.90	8.2×10^5	9.1×10^4	9.0
		2-MeTHF (77)	484, 517	445	4.1				
8a		PMMA (298)	495	430	1.1	0.87	7.9×10^5	1.2×10^5	6.7
		powder (298)	501	465	0.5				
	492	2-MeTHF (298)	494	440	0.2	0.56	2.8×10^6	2.2×10^6	1.3
		2-MeTHF (77)	475, 506	440	5.6				
8b		PMMA (298)	497	440	1.0	0.72	7.4×10^5	2.9×10^5	2.6
	477	2-MeTHF (298)	489	430	0.6	0.74	1.3×10^6	4.3×10^5	2.9
		2-MeTHF (77)	465, 496	430	3.9				
10a		PMMA (298)	636	480	0.2	0.34	1.7×10^6	3.3×10^6	0.5
	651	2-MeTHF (298)	632	485	0.9	0.40	4.4×10^5	6.7×10^5	0.7
		2-MeTHF (77)	637	490	2.7				

[a]Predicted from TD-DFT calculations in THF at 298 K. [b]Calculated according to the equations $k_r = \phi/\tau$ and $k_{nr} = (1 - \phi)/\tau$, where k_r is the radiative rate constant, k_{nr} is the nonradiative rate constant, ϕ is the quantum yield, and τ is the excited-state lifetime

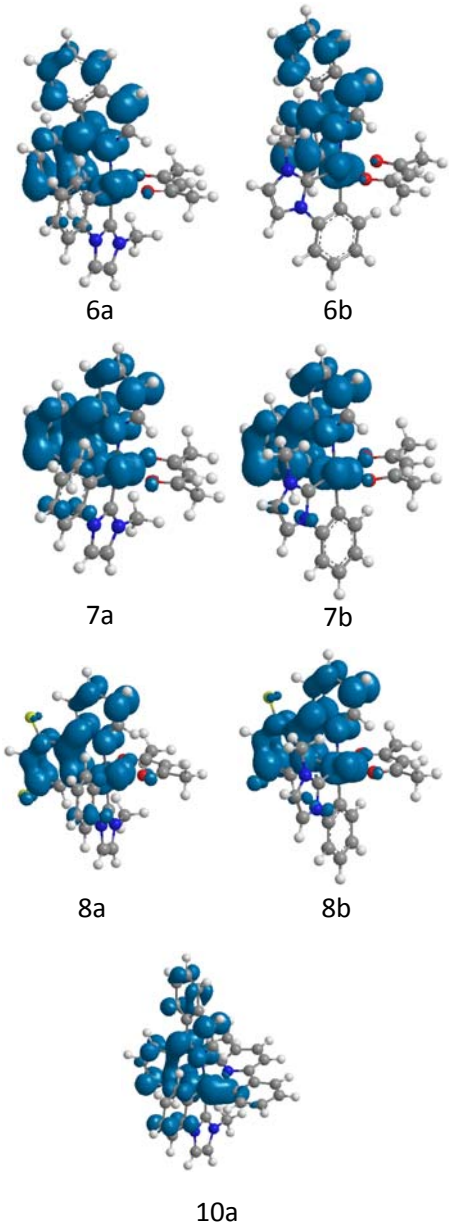

Figure 11. DFT calculated spin density of **6a**–**8b** and **10a** at 0.003 au contour level.

Electroluminiscence Properties of an OLED Device Based on 6a. In order to study the influence of the replacement of a *C*,*N*-ligand by a cyclometalated aryl-NHC group on the applicability of luminescent materials derived from heteroleptic iridium(III) complexes, we have compared an OLED device based on complex **6a**, containing cyclometalated phenylisoquinoline

and a cyclometalated aryl-NHC ligand, with another one based on Ir{κ^2-*C*,*N*-(C_6H_4-isoqui)}$_2$(κ^2-*O*,*O*-acac) (**11**) bearing two cyclometalated phenylisoquinoline groups. They were fabricated by high vacuum (< 10^{-7} Torr) thermal evaporation. Their structure and the formulas of the compounds used in the fabrication are depicted in Figure 12. The devices consist in an anode electrode (1150 Å) of indium tin oxide (ITO); a hole injection layer (HIL; 100 Å) of HAT-CN; a hole transporting layer (HTL; 450 Å) of NPD; an emissive layer (EML; 400 Å) containing $BAlq_2$ as a host doped with either compound **6a** or the comparative compound **11** as emitter (9%); Alq_3 as electron transporting layer (ETL; 450 Å); LiF as electron injection layer (EIL; 10 Å); and aluminum as cathode (1000 Å). Both devices were encapsulated with a glass lid sealed with an epoxy resin in a nitrogen filled glove box (< 1 ppm of H_2O and O_2) immediately after fabrication, and a moisture getter was incorporated inside the package.

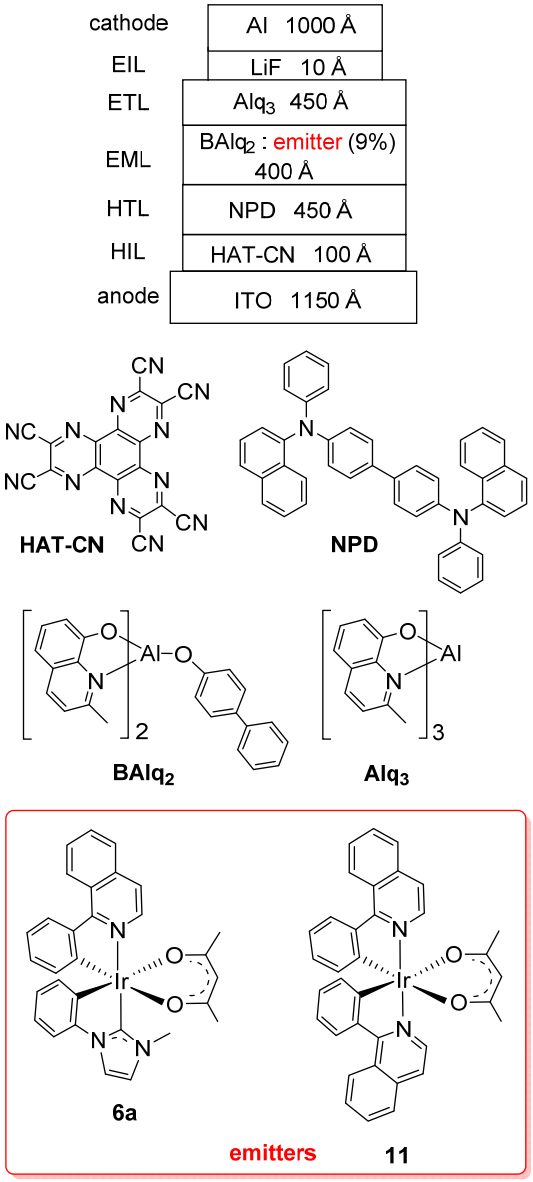

Figure 12. OLED construction and chemical structures of the compounds used in the devices.

The electroluminescence (EL) and current density-voltage-luminance (J-V-L) characteristics of the devices were tested upon their fabrication. The performance data of both devices are presented in Table 4 and Figure 13. Current density-voltage-luminance scan was stopped at 190 mA/cm^2 due to instrument compliance. At this point, the device with compound **6a** demonstrated ~15 000 cd/m^2 whereas that with comparative compound **11** displayed ~10 000 cd/m^2.

Table 4. Summary of the Performances of the Devices Based on 6a and Comparative Compound 11

	1931 CIE				at 1000 cd/m^2						at 80 mA/cm^2	
emitter (9%)	CIE *x*	CIE *y*	λ_{max} (nm)	fwhm[a] (nm)	voltage (V)	LE[b] (cd/A)	EQE[c] (%)	PE[d] (lm/W)	LE/EQE (cd/A /%)	$LT_{95\%}$[e] (h)	L_0[f] (cd/m^2)	$LT_{95\%}$[e] (h)
6a	0.656	0.343	616	93	7.4	13.0	12.9	5.5	1.01	3600	8023	56
11	0.681	0.317	631	84	8.3	8.0	11.5	3.0	0.70	3500	5125	133

[a]Full width at half-maximum of the emission peak in the electroluminescence spectrum. [b]Luminous efficacy. [c]External quantum efficiency. [d]Power efficacy. [e]Lifetime as the time the luminance drops to 95% of its initial value. [f]Initial luminance.

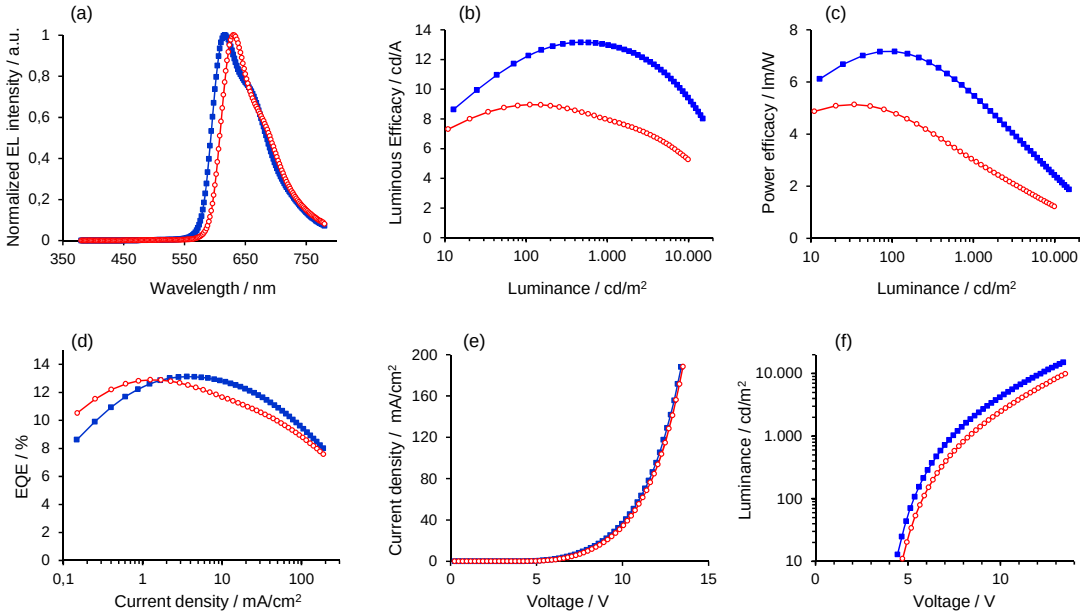

Figure 13. Plots of (a) electroluminescence spectra, (b) luminous efficacy vs luminance, (c) power efficacy vs luminance, (d) external quantum efficiency vs current density, (e) current density vs voltage, and (f) luminance vs voltage for the OLED devices based on complex **6a** (blue ■) and comparative derivative **11** (red ○).

The electroluminescence spectrum (EL) of compound **6a** device shows a maximum at a wavelength of 616 nm which is consistent with the photoluminescence (PL) measurements. It is

15 nm blue shifted with regard to that of **11** (Figure 13a). This explains the much higher luminous efficacy (LE) (Figure 13b) and power efficacy (PE) (Figure 13c) of the **6a** device due to significant emission shift to the higher human eye photopic response region and the higher luminous efficacy/external quantum efficiency (LE/EQE) ratio (1.01 for **6a** vs 0.70 for **11**; Table 4). No significant spectral change was observed at increased luminance for both emitters due to well confined excitons in the devices emissive layer. External quantum efficiency of both devices is similar at low current density (Figure 13d). However; compound **6a** device demonstrates much less efficiency roll-off with current density increase, indicating a better charge balance in the device emissive layer. Figure 13e reveals current density-voltage characteristics similar for both compounds; which suggests similar charge transport mechanism with both emitters. The luminance increase with the voltage for **6a** with regard to **11** (Figure 13f) is mostly explained by the spectrum blue shift and higher LE/EQE ratio for the former (Table 4).

Devices were life tested at accelerated conditions of current density 80 mA/cm^2 at room temperature. The time at which the luminance drops to 95% of its initial value ($LT_{95\%}$) at constant luminance (1000 cd/m^2) was calculated assuming acceleration factor 2. The device lifetime at the same current density was over 2 times lower for **6a** ($LT_{95\%}$ 56 h for **6a** vs $LT_{95\%}$ 133 h for **11**), which could be explained by a significantly higher exciton energy for **6a** due to the spectral blue shift. It is well known that higher energy exciton results in more damage to the device.[31] However, lifetimes at the same luminance are similar ($LT_{95\%}$ at 1000 cd/m^2 is 3600 h for **6a** and 3500 h for **11**), as a consequence of the higher initial luminance at life-tested current density for the **6a** device.

Comparison proves that the performance of **6a** device is superior or similar to the device performance of **11**; i.e., the replacement of a *C*,*N*-ligand by a cyclometalated aryl-NHC group

gives rise to higher luminous efficacy and power efficacy. This demonstrates that tris-heteroleptic complexes can be used as emitters in OLED devices with various applications including displays, lightning, etc in spite of their high tendency to ligand redistribution.

Concluding Remarks

This paper reveals efficient procedures to prepare tris-heteroleptic [3b+3b'+3b"] iridium(III) complexes containing a cyclometalated aryl-NHC, a cyclometalated aryl-N-heterocycle, and an acac or a second cyclometalated aryl-N-heterocycle. The procedures involve the transmetalation of the NHC ligand from a silver adduct to the metal center of the known dimer $[Ir(\mu\text{-}Cl)(COD)]_2$, to afford a square-planar IrCl(COD)(NHC) synthetic intermediate. The later promotes the NHC- and N-heterocycle-supported *ortho*-CH bond activation of the phenyl substituents of the coordinated NHC ligand and an external N-heterocycle to form iridium(III) dimers of the type $[Ir(\mu\text{-}Cl)(3b)(3b')]_2$, bearing both cyclometalated aryl-NHC (3b) and cyclometalated aryl-N-heterocycle (3b') ligands. Treatment of these dimers with Kacac yields the desired [3b+3b'+3b''] complexes. The replacement of acac by the second cyclometalated aryl-N-heterocycle (3b") takes place by transmetalation from a pinacolboryl group via a bis(aquo) intermediate. The marked differences between the ligands, from an electronic point of view, produce a noticeable stability of the heteroleptic coordination sphere of the iridium(III) center, preventing ligand redistribution reactions.

The new complexes are phosphorescent. The emission can be tuned in a wide range of wavelengths by means of the appropriate combination of the substituents of the ligands. In comparison with [3b+3b+3b'] heteroleptic iridium(III) complexes containing two cyclometalated *C*,*N*-ligands, a significant increase of the quantum yield is observed in the new [3b+3b'+3b'']

emitters. A notable improvement with regard to those containing two cyclometalated *C*,*N*-ligands is also achieved from the point of view of their applicability to the fabrication of OLED devices. The introduction of the cyclometalated aryl-NHC group allows reaching a brightness of 1000 cd/m^2 at a lower voltage and appears to give rise to higher luminous efficacy and power efficacy.

In conclusion, a new class of phosphorescent tris-heteroleptic iridium(III) complexes has been discovered. The new emitters are more stable toward ligand redistribution reactions and appear to display better properties to the fabrication of OLED devices from their applicability point of view.

Experimental Section

General Information. The reactions were carried out under moisture- and oxygen-free atmosphere using dried solvents and Schlenk-tube techniques. Instrumental methods, X-ray information, and DFT computational details are given in the Supporting Information. In the NMR spectra, chemical shifts (expressed in parts per million) are referenced to residual solvent peaks (^{1}H, ^{13}C{^{1}H}) or external $CFCl_3$ (^{19}F) and coupling constants (*J*) are given in hertz. 2-(2-pinacolborylphenyl)-5-methylpyridine was provided by UDC. [Ir(μ-Cl)(COD)]$_2$ (**1**)[32] and 1-phenyl-3-methylimidazolium iodide [PhMeImH]I[33] were prepared by previously published methods.

Preparation of IrCl(COD)(PhMeIm) (2). A black suspension of silver oxide (139.5 mg, 0.596 mmol) and 1-phenyl-3-methylimidazolium iodide [PhMeImH]I (340.8 mg, 1.19 mmol) in CH_2Cl_2 (15 mL) was stirred for two hours in the presence of 4 Å molecular sieves (400 mg) in the absence of light; during this time, the mixture evolved to a beige suspension. Then, [Ir(μ-Cl)(COD)]$_2$ (**1**, 400 mg, 0.596 mmol) was added, resulting in a yellow suspension. After 20 min,

the yellow solution was extracted from the silver salts and concentrated in *vacuo* to ca. ~0.5 mL. Pentane (10 mL) was added and a yellow solid precipitated. The solid was washed with pentane (3 × 6 mL) yielding **2**. Yield: 543.5 mg (92%). Anal. Calcd. for $C_{18}H_{22}ClIrN_2$: C, 43.76; H, 4.49; N, 5.67. Found: C, 43.65; H, 4.61; N, 5.34. ^{1}H NMR (300.13 MHz, CD_2Cl_2, 298 K): δ 8.03-8.00 (m, 2H, CH), 7.52-7.41 (m, 3H, CH), 7.19 (d, $^3J_{H-H}$ = 1.7, 1H, CH), 7.04 (d, $^3J_{H-H}$ = 1.7, 1H, CH), 4.61-4.54 (m, 1H, CH=), 4.43-4.37 (m, 1H, CH=), 4.05 (s, 3H, CH_3), 2.92-2.86 (m, 1H, CH=), 2.27-2.21 (m, 1H, CH=), 2.19-2.12 (m, 2H, CH_2), 1.96-1.84 (m, 1H, CH_2), 1.66-1.48 (m, 3H, CH_2), 1.44-1.31 (m, 1H, CH_2), 1.27-1.15 (m, 1H, CH_2). ^{13}C{^{1}H} + HMBC + HSQC NMR (75.47 MHz, CD_2Cl_2, 298K): δ 181.2 (NCN), 140.6 (Cq), 129.0 (CH), 128.1 (CH), 125.5 (CH), 122.9 (CH), 121.4 (CH), 83.9 (CH=), 83.6 (CH=), 52.1 (CH=), 51.9 (CH=), 38.4 (NCH_3), 34.3 (CH_2), 32.9 (CH_2), 29.8 ($2CH_2$).

Preparation of [Ir(μ-Cl){κ^2-*C*,*C*-(C_6H_4-ImMe)}{κ^2-*C*,*N*-(C_6H_4-isoqui)}]$_2$ (3a and 3b). 1-Phenylisoquinoline (207.3 mg, 1.01 mmol) was added to a suspension of **2** (500 mg, 1.01 mmol) in methanol (6 mL) and the resulting yellow suspension was refluxed for 5 days. The resulting orange suspension was decanted from the orange solution and washed with MeOH (3 × 4 mL) yielding a mixture of two isomers in a 1:1 ratio. Yield: 416 mg (70%). X-ray quality crystals of **3a** were grown by layering a solution of **3a** and **3b** in CH_2Cl_2 with toluene. Spectroscopic data of both isomers **3a** and **3b**: ^{1}H NMR (500.13 MHz, CD_2Cl_2, 298 K): δ 9.55-9.53 (m, 2H, CH), 9.07-9.06 (m, 2H, CH), 8.97-8.94 (m, 4H, CH), 8.17-8.09 (m, 6H, CH), 8.00-7.98 (m, 2H, CH), 7.89-7.84 (m, 4H, CH), 7.79-7.75 (m, 4H, CH), 7.63-7.62 (m, 4H, CH), 7.59-7.57 (m, 2H, CH), 7.19-7.18 (m, 2H, CH), 7.04-7.01 (m, 4H, CH), 6.99-6.98 (m, 2H, CH), 6.96-6.95 (m, 2H, CH), 6.91-6.86 (m, 4H, CH), 6.77-6.62 (m, 8H, CH), 6.38-6.28 (m, 8H, CH), 5.84-5.81 (m, 4H, CH), 3.85 (s, 6H, NCH_3), 3.25 (s, 6H, NCH_3). ^{13}C{^{1}H} + HMBC + HSQC NMR (125.76 MHz, CD_2Cl_2, 298

K): δ 167.6 (Cq), 167.2 (Cq), 163.8 (NCN), 163.4 (NCN), 149.6 (Cq), 148.5 (Cq), 147.2 (Cq), 147.1 (Cq), 145.4 (Cq), 145.2 (Cq), 142.7 (CH), 141.9 (CH), 137.9 (Cq), 137.8 (Cq), 136.6 (CH), 136.3 (CH), 132.7 (CH), 132.4 (CH), 131.4 (CH), 131.2 (CH), 130.8 (Cq), 130.6 (Cq), 130.4 (CH), 130.3 (CH), 129.9 (CH), 129.7 (CH), 128.1 (CH), 128.0 (CH), 127.9 (CH), 127.8 (CH), 127.6 (CH), 127.5 (CH), 126.6 (Cq), 126.5 (Cq), 124.3 (CH), 124.1 (CH), 122.6 (CH), 122.4 (CH), 122.0 (CH), 121.9 (CH), 120.9 (CH), 120.7 (CH), 120.2 (CH), 119.9 (CH), 115.8 (CH), 115.6 (CH), 110.8 (CH), 110.7 (CH), 37.2 (NCH_3), 36.1 (NCH_3).

Preparation of [Ir(μ-Cl){κ^2-*C*,*C*-(C_6H_4-ImMe)}{κ^2-*C*,*N*-(C_6H_4-py)}]$_2$ (4a and 4b). 2-Phenylpyridine (236 μL, 1.622 mmol) was added to a suspension of **2** (800 mg, 1.622 mmol) in methanol (15 mL) and the resulting yellow suspension was refluxed for 3 days. The resulting pale yellow suspension was decanted from the orange solution and washed with MeOH (3 × 4 mL) yielding a mixture of two isomers in a 1.8:1.0 ratio. Yield: 690.4 mg (79%). Spectroscopic data of isomer **4a**: ^{1}H NMR (500.13 MHz, CD_2Cl_2, 298 K): δ 9.56-9.54 (m, 2H, CH), 8.04-7.99 (m, 4H, CH), 7.61-7.57 (m, 4H, CH), 7.26-7.23 (m, 2H, CH), 7.06-6.98 (m, 4H, CH), 6.82-6.73 (m, 4H, CH), 6.66-6.61 (m, 2H, CH), 6.43-6.39 (d, 2H, CH), 6.20-6.19 (m, 2H, CH), 5.88-5.85 (m, 2H, CH), 3.47 (s, 6H, NCH_3). $^{13}C\{^1H\}$ + HMBC + HSQC NMR (125.76 MHz, CD_2Cl_2, 298 K): δ 166.6 (Cq), 163.1 (NCN), 149.8 (CH), 147.3 (Cq), 146.0 (Cq), 143.8 (Cq), 137.9 (CH), 136.5 (CH), 132.1 (CH), 130.6 (Cq), 130.1 (CH), 124.5 (CH), 124.3 (CH), 122.4 (CH), 122.1 (CH), 122.0 (CH), 121.4 (CH), 119.3 (CH), 115.8 (CH), 110.8 (CH), 37.5 (NCH_3). Spectroscopic data of isomer **4b**: ^{1}H NMR (500.13 MHz, CD_2Cl_2, 298 K): δ 9.33-9.32 (m, 2H, CH), 7.98-7.94 (m, 2H, CH), 7.92-7.88 (m, 2H, CH), 7.61-7.57 (m, 4H, CH), 7.18-7.17 (m, 2H, CH), 7.06-6.98 (m, 4H, CH), 6.82-6.73 (m, 4H, CH), 6.66-6.61 (m, 2H, CH), 6.43-6.39 (m, 2H, CH), 6.14-6.12 (m, 2H, CH), 5.88-5.85 (m, 2H, CH), 3.79 (s, 6H, NCH_3). $^{13}C\{^1H\}$ + HMBC +

HSQC NMR (125.76 MHz, CD_2Cl_2, 298K) δ 166.1 (Cq), 163.6 (NCN), 151.1 (CH), 147.3 (Cq), 144.9 (Cq), 143.9 (Cq), 137.6 (CH), 136.1 (CH), 132.4 (CH), 130.7 (Cq), 130.0 (CH), 124.5 (CH), 124.4 (CH), 123.0 (CH), 122.5 (CH), 122.1 (CH), 121.5 (CH), 119.3 (CH), 116.0 (CH), 111.0 (CH), 36.1 (NCH_3). Two Cq resonances are not observed, due to overlapping with other peaks.

Preparation of [Ir(μ-Cl){κ^2-*C*,*C*-(C_6H_4-ImMe)}{κ^2-*C*,*N*-($C_6F_2H_2$-py)}]$_2$ (5a and 5b). Methanol (15 mL) was added to a mixture of **2** (500 mg, 1.01mmol) and 2,4-difluorophenylpyridine (dfppy) (160 μL, 1.01 mmol) and the resulting yellow suspension was refluxed for 3 days. The resulting pale yellow suspension was decanted from the orange solution and washed with MeOH (3 × 4 mL) yielding a mixture of two complexes in a 1.8:1.0 ratio. Yield: 469.4 mg (81%). Spectroscopic data of isomer **5a**: ^{1}H NMR (500.13 MHz, CD_2Cl_2, 298 K): δ 9.53-9.51 (m, 2H, CH), 8.41-8.39 (m, 2H, CH), 8.03-7.98 (m, 2H, CH), 7.62 (d, $^3J_{H-H}$ = 2.2, 2H, CH), 7.28-7.25 (m, 2H, CH), 7.06-7.02 (m, 4H, CH), 6.80-6.77 (m, 2H, CH), 6.46-6.43 (m, 2H, CH), 6.34-6.29 (m, 2H, CH), 5.83-5.81 (m, 2H, CH), 5.70-5.68 (m, 2H, CH), 3.45 (s, 6H, NCH_3). ^{13}C{^{1}H} + HMBC + HSQC NMR (125.76 MHz, CD_2Cl_2, 298 K): δ 163.7 (d, $^2J_{C-F}$ = 6.9, Cq), 163.2 (dd, $^1J_{C-F}$ = 253.3, $^3J_{C-F}$ = 12.5, CF), 162.1 (s, NCN), 161.2 (dd, $^1J_{C-F}$ = 258.2, $^3J_{C-F}$ = 13.1, CF), 150.4 (d, $^3J_{C-F}$ = 7.1, Cq), 149.8 (s, CH), 147.0 (s, Cq), 138.5 (s, CH), 132.0 (s, CH), 129.4 (s, Cq), 129.1 (s, CH), 128.0 (br, Cq), 124.4 (s, CH), 123.4 (d, $^4J_{C-F}$ = 21.4, CH), 122.7 (s, CH), 122.4 (s, CH), 118.3 (dd, d, $^2J_{C-F}$ = 17.3, $^4J_{C-F}$ = 2.8, CH), 116.2 (s, CH), 111.2 (s, CH), 97.6 (dd, $^2J_{C-F}$ = 27.2, $^2J_{C-F}$ = 27.2, CH), 37.4 (s, NCH_3). ^{19}F{^{1}H} NMR (282.33 MHz, CD_2Cl_2, 298 K): δ -110.0 (d, $^4J_{F-F}$ = 10.0, 1F, CF), -110.4 (d, $^4J_{F-F}$ = 10.0, 1F, CF). Spectroscopic data of isomer **5b**: ^{1}H NMR (500.13 MHz, CD_2Cl_2, 298 K): δ 9.32-9.30 (m, 2H, CH), 8.37-8.35 (m, 2H, CH), 7.95-7.91 (m, 2H, CH), 7.64 (d, $^3J_{H-H}$ = 2.2, 2H, CH), 7.20-7.19 (m, 2H, CH), 7.06-7.02 (m, 4H,

CH), 6.80-6.77 (m, 2H, CH), 6.46-6.43 (m, 2H, CH), 6.34-6.29 (m, 2H, CH), 5.83-5.81 (m, 2H, CH), 5.63-5.61 (m, 2H, CH), 3.77 (s, 6H, NCH_3). $^{13}C\{^1H\}$ + HMBC + HSQC NMR (125.76 MHz, CD_2Cl_2, 298 K): δ 163.2 (d, $^2J_{C-F}$ = 6.6, Cq), 162.5 (m, assigned indirectly through HMBC, CF), 162.5 (s, NCN), 160.5 (m, assigned indirectly through HMBC, CF), 151.0 (s, CH), 149.4 (d, $^3J_{C-F}$ = 7.0, Cq), 147.0 (s, CH), 138.2 (s, CH), 132.3 (s, CH), 129.4 (s, Cq), 128.2 (s, CH), 128.1 (br, Cq), 123.4 (d, $^4J_{C-F}$ = 21.5, CH), 122.8 (s, CH), 122.7 (s, CH), 118.1 (dd, d, $^2J_{C-F}$= 17.6, $^4J_{C-F}$= 2.7, CH), 116.3 (s, CH), 111.3 (s, CH), 97.6 (dd, $^2J_{C-F}$ = 27.2, $^2J_{C-F}$ = 27.2, CH), 36.1 (s, NCH_3). One resonance is not observed due to overlapping. $^{19}F\{^1H\}$ NMR (282.33 MHz, CD_2Cl_2, 298 K): δ -110.1 (d, $^4J_{H-H}$ = 9.9, 1F, CF), -110.7 (d, $^4J_{H-H}$ = 9.9, 1F, CF).

Preparation of Ir{κ^2-*C*,*C*-(C_6H_4-ImMe)}{κ^2-*C*,*N*-(C_6H_4-isoqui)}{κ^2-*O*,*O*-(acac)} (6a and 6b). *Method **a***: An orange suspension of **3a** and **3b** (357 mg, 0.303 mmol) in THF (12 mL) in the presence of Kacac (92.2 mg, 0.666 mmol) was stirred at 60 ºC for 90 min. The resulting red solution was concentrated to dryness and purified by column chromatography (silicagel 230-400 mesh, toluene with a gradual increase of the polarity with CH_2Cl_2) yielding **6a** (red) and **6b** (orange). Yield: **6a**: 93.4 mg (24%), **6b**: 43.7 mg (11%). *Method **b***: THF (8 mL) and a Kacac solution in MeOH (3.46 mL, 0.258 M) were added to **3a** and **3b** (357 mg, 0.303 mmol). The resulting red suspension was stirred for 90 min at 60 ºC and then it was concentrated to dryness. The resulting residue was dissolved in the minimal amount of dichloromethane and purified by chromatography column (silicagel 230-400 mesh, toluene with a gradual increase of the polarity with CH_2Cl_2). **6a**: Yield: 260 mg (66%). **6a**: X-ray quality crystals were grown by layering a solution of this complex in CH_2Cl_2 with pentane. Anal. Calcd. for $C_{30}H_{26}IrN_3O_2$: C, 55.20; H, 4.02; N, 6.44. Found: C, 54.87; H, 3.66; N, 6.46. HRMS (electrospray, *m/z*) calcd for $C_{30}H_{26}IrN_3O_2$ $[M]^+$: 653.1650; found: 653.1652. ^1H NMR (300.13 MHz, CD_2Cl_2, 298 K): δ 8.96-

8.93 (m, 1 H, CH), 8.39-8.37 (m, 1H, CH), 8.18-8.15 (m, 1H, CH), 7.98-7.96 (m, 1H, CH), 7.78-7.70 (m, 3H, CH), 7.49 (d,$^{3}J_{H\text{-}H}$ = 2.1, 1H, CH), 7.06 (d, $^{3}J_{H\text{-}H}$ = 2.1, 1H, CH), 7.06-7.03 (m, 1H, CH), 6.93-6.88 (m, 1H, CH), 6.80-6.68 (m, 2H, CH), 6.47-6.43 (m, 2H, CH), 6.16-6.14 (m, 1H, CH), 5.30 (s, 1H, CH acac), 3.83 (s, 3H, NCH_3), 1.86 (s, 3H, CH_3 acac), 1.65 (s, 3H, CH_3 acac). $^{13}C\{^{1}H\}$ + HMBC + HSQC NMR (75.47 MHz, CD_2Cl_2, 298 K): δ 185.6 (CO acac), 185.3 (CO acac), 167.4 (Cq), 165.4 (NCN), 151.6 (Cq), 148.8 (Cq), 146.7 (Cq), 139.4 (CH), 138.5 (CH), 138.2 (Cq), 135.0 (CH), 131.6 (Cq), 131.2 (CH), 130.5 (CH), 129.6 (CH), 128.2 (CH), 127.9 (CH), 127.8 (CH), 126.8 (Cq), 124.2 (CH), 121.8 (CH), 121.6 (CH), 120.7 (CH), 120.6 (CH), 115.2 (CH), 110.7 (CH), 101.5 (CH acac), 35.7 (NCH_3), 28.9 and 28.4 (both CH_3 acac). **6b:** Anal. Calcd. for $C_{30}H_{26}IrN_3O_2$: C, 55.20; H, 4.02; N, 6.44. Found: C, 54.94; H, 3.69; N, 6.14. ^{1}H NMR (300.13 MHz, CD_2Cl_2, 298 K): δ 8.97-8.95 (m, 1 H, CH), 8.47-8.45 (m, 1H, CH), 8.18-8.15 (m, 1H, CH), 7.97-7.94 (m, 1H, CH), 7.78-7.70 (m, 2H, CH), 7.63-7.61 (m, 1H, CH), 7.39 (d, $^{3}J_{H\text{-}H}$ = 2.1, 1H, CH), 7.36-7.33 (m, 1H, CH), 7.24-7.21 (m, 1H, CH), 7.10-7.05 (m, 1H, CH), 6.98-6.89 (m, 2H, CH), 6.69-6.63 (m, 2H, CH), 6.52-6.49 (m, 1H, CH), 5.19 (s, 1H, CH acac), 2.98 (s, 3H, NCH_3), 1.80 (s, 3H, CH_3 acac), 1.64 (s, 3H, CH_3 acac). $^{13}C\{^{1}H\}$ + HMBC + HSQC NMR (75.47 MHz, CD_2Cl_2, 298 K): δ 184.1 (CO acac), 184.0 (CO acac), 167.2 (Cq), 154.6 (NCN), 148.1 (Cq), 147.7 (Cq), 147.3 (Cq), 144.0 (Cq), 140.0 (CH), 138.7 (CH), 138.1 (Cq), 134.2 (CH), 131.1 (CH), 130.2 (CH), 128.8 (CH), 128.2 (CH), 127.9 (CH), 127.9 (CH), 127.0 (Cq), 124.8 (CH), 121.9 (CH), 121.3 (CH), 120.9 (CH), 120.4 (CH), 114.9 (CH), 110.9 (CH), 100.9 (CH acac), 35.6 (NCH_3), 28.7 and 28.3 (both CH_3 acac).

Preparation of Ir{κ^2-*C*,*C*-(C_6H_4-ImMe)}{κ^2-*C*,*N*-(C_6H_4-py)}{κ^2-*O*,*O*-(acac)} (7a and 7b). THF (15 mL) was added to a mixture of **4a** and **b** (400 mg, 0.37 mmol) and Kacac (112 mg, 0.81 mmol) and the yellow suspension was stirred for 90 min at 60 ºC. The resulting yellow solution

was concentrated to dryness. The resulting residue was dissolved in the minimal amount of dichloromethane and was purified by column chromatography (silicagel 230-400 mesh, CH_2Cl_2/toluene 1/10 as eluent) yielding **7a** (yellow) and **7b** (yellow). **7a**: Yield: 191.2 mg (43%). X-ray quality crystals were grown by layering a solution of this complex in CH_2Cl_2 with pentane. Anal. Calcd. for $C_{26}H_{24}IrN_3O_2$: C, 51.81; H, 4.01; N, 6.97. Found: C, 51.63; H, 3.78; N, 6.95. ^{1}H NMR (400.13 MHz, CD_2Cl_2, 298 K): δ 8.45-8.44 (m, 1 H, CH), 7.92-7.90 (m, 1H, CH), 7.85-7.81 (m, 1H, CH), 7.586-7.57 (m, 1H, CH), 7.47 (m, 1H, CH), 7.31-7.28 (m, 1H, CH), 7.04-7.01 (m, 2H, CH), 6.83-6.76 (m, 2H, CH), 6.69-6.65 (m, 1H, CH), 6.53-6.49 (m, 1H, CH), 6.30-6.28 (m, 1H, CH), 6.24-6.22 (m, 1H, CH), 5.30 (s, 1H, CH acac), 3.80 (s, 3H, NCH_3), 1.84 (s, 3H, CH_3 acac), 1.68 (s, 3H, CH_3 acac). ^{13}C{^{1}H} + HMBC + HSQC NMR (100.61 MHz, CD_2Cl_2, 298K): δ 185.5 (CO acac), 185.2 (CO acac), 166.4 (Cq), 164.8 (NCN), 148.8 (Cq), 147.5 (Cq), 147.1 (CH), 145.1 (Cq), 138.2 (CH), 138.0 (CH), 134.6 (CH), 131.5 (Cq), 129.6 (CH), 124.4 (CH), 124.2 (CH), 122.5 (CH), 121.6 (CH), 121.5 (CH), 121.0 (CH), 119.2 (CH), 115.2 (CH), 110.6 (CH), 101.4 (CH acac), 35.6 (NCH_3), 28.8 and 28.4 (both CH_3 acac). **7b**: Yield: 93.0 mg (21%). X-ray quality crystals were grown by layering a solution of this complex in CH_2Cl_2 with pentane. Anal. Calcd. for $C_{26}H_{24}IrN_3O_2$: C, 51.81; H, 4.01; N, 6.97. Found: C, 51.95; H, 4.15; N, 6.81. HRMS (electrospray, *m/z*) calcd for $C_{26}H_{24}IrN_3O_2$ $[M]^+$: 603.1498; found: 603.1493. ^{1}H NMR (400.13 MHz, CD_2Cl_2, 298 K): δ 8.53-8.51 (m, 1H, CH), 7.96-7.94 (m, 1H, CH), 7.84-7.80 (m, 1H, CH), 7.61-7.60 (m, 1H, CH), 7.35-7.33 (m, 2H, CH), 7.29-7.26 (m, 1H, CH), 7.19-7.17 (m, 1H, CH), 7.07-7.03 (m, 1H, CH), 6.96-6.93 (m, 1H, CH), 6.84-6.80 (m, 1H, CH), 6.65-6.61 (m, 2H, CH), 6.38-6.37 (m, 1H, CH), 5.24 (s, 1H, CH acac), 2.96 (s, 3H, NCH_3), 1.79 (s, 3H, CH_3 acac), 1.73 (s, 3H, CH_3 acac). ^{13}C{^{1}H} + HMBC + HSQC NMR (100.61 MHz, CD_2Cl_2, 298 K): δ 184.0 (CO acac), 183.9 (CO acac), 166.4 (Cq), 154.0 (NCN), 148.0 (Cq), 147.8 (CH),

145.7 (Cq), 144.7(Cq), 143.4 (Cq), 138.5 (CH), 138.0 (CH), 134.1 (CH), 129.1 (CH), 124.8 (CH), 124.2 (CH), 122.4 (2CH), 121.7 (CH), 121.4 (CH),119.5 (CH), 114.8 (CH), 110.7 (CH), 101.0 (CH acac), 35.4 (NCH_3), 28.7 and 28.4 (CH_3 acac).

Preparation of Ir{κ^2-*C*,*C*-(C_6H_4-ImMe)}{κ^2-*C*,*N*-($C_6F_2H_2$-py)}{κ^2-*O*,*O*-(acac)} (8a and 8b). THF (15 mL) was added to a mixture of **5a** and **b** (400 mg, 0.35 mmol) and Kacac (105.8 mg, 0.77 mmol) and the yellow suspension was stirred at 60ºC for 90 min. The resulting yellow solution was concentrated to dryness. The resulting residue was dissolved in the minimal amount of dichloromethane and was purified by chromatography (silicagel 230-400 mesh, CH_2Cl_2/toluene 1/10 as eluent) yielding **8a** (yellow) and **8b** (yellow). **8a**: Yield: 268.5 mg (60%). Anal. Calcd. for $C_{26}H_{22}F_2IrN_3O_2$: C, 48.89; H, 3.47; N, 6.58. Found: C, 48.67; H, 3.24; N, 6.55. ^{1}H NMR (400.13 MHz, CD_2Cl_2, 298 K): δ 8.46-8.45 (m, 1H, CH), 8.28-8.26 (m, 1H, CH), 7.88-7.84 (m, 1H, CH), 7.48 (d, $^3J_{H-H}$ = 2.1, 1H, CH), 7.33-7.30 (m, 1H, CH), 7.05-7.04 (m, 2H, CH), 6.83-6.79 (m, 1H, CH), 6.56-6.52 (m, 1H, CH), 6.33-6.27 (m, 1H, CH), 6.19-6.17 (m, 1H, CH), 5.81-5.79 (m, 1H, CH), 5.31 (s, 1H, CH acac), 3.80 (s, 3H, NCH_3), 1.83 (s, 3H, CH_3 acac), 1.69 (s, 3H, CH_3 acac). ^{13}C{^{1}H} + HMBC + HSQC NMR (100.61 MHz, CD_2Cl_2, 298K): δ 185.6 (s, CO acac), 185.4 (s, CO acac), 163.8 (s, NCN), 163.3 (d, $^2J_{C-F}$ = 6.6, Cq), 163.2 (dd, $^1J_{C-F}$ = 254.8, $^3J_{C-F}$ = 13.6, CF), 161.3 (dd, $^1J_{C-F}$ = 254.8, $^3J_{C-F}$ = 13.6, CF), 153.1 (d, $^2J_{C-F}$ = 6.7, Cq), 148.6 (s, Cq), 147.1 (s, CH), 138.6 (s, CH), 134.6 (s, CH), 130.4 (s, Cq), 129.0 (dd, $^3J_{C-F}$ = 3.1, $^3J_{C-F}$ = 3.1, Cq), 124.4 (s, CH), 123.3 (d, $^4J_{C-F}$ = 20.5, CH), 122.5 (s, CH), 122.0 (s, CH), 121.9 (s, CH), 119.8 (dd, d, $^2J_{C-F}$ = 16.3, $^4J_{C-F}$ = 2.8, CH), 115.4 (s, CH), 110.9 (s, CH), 101.5 (s, CH acac), 97.0 (dd, $^2J_{C-F}$ = 27.2, $^2J_{C-F}$ = 27.2, CH), 35.6 (s, NCH_3), 28.7 and 28.4 (both s, CH_3 acac). ^{19}F{^{1}H} NMR (282.33 MHz, CD_2Cl_2, 298 K): δ -110.9 (d, $^4J_{F-F}$ = 9.8, 1F, CF), -111.2 (d, $^4J_{F-F}$ = 9.8, 1F, CF). **8b**: Yield: 45.2 mg (10 %). Anal. Calcd. for $C_{26}H_{22}F_2IrN_3O_2$: C, 48.89; H, 3.47; N, 6.58.

Found: C, 48.57; H, 3.52; N, 6.89. ^{1}H NMR (300.13 MHz, CD_2Cl_2, 298 K): δ 8.55-8.53 (m, 1H, CH), 8.33-8.29 (m, 1H, CH), 7.88-7.82 (m, 1H, CH), 7.38 (d, $^{3}J_{H-H}$ = 2.1, 1H, CH), 7.33-7.28 (m, 2H, CH), 7.22-7.19 (m, 1H, CH), 7.11-7.05 (m, 1H, CH), 6.99-6.94 (m, 1H, CH), 6.68 (d, $^{3}J_{H-H}$ = 2.1, 1H, CH), 6.32 (ddd, $^{3}J_{H-F}$ = 13.1, $^{3}J_{H-F}$ = 9.2, $^{4}J_{H-H}$ = 2.4, 1H, CH), 5.90 (dd, $^{3}J_{H-F}$ = 9.3, $^{4}J_{H-H}$ = 2.4, 1H, CH), 5.26 (s, 1H, CH acac), 2.98 (s, 3H, NCH_3), 1.78 (s, 3H, CH_3 acac), 1.74 (s, 3H, CH_3 acac). $^{13}C\{^{1}H\}$ + HMBC + HSQC NMR (75.47 MHz, CD_2Cl_2, 298 K): δ 184.2 (s, CO acac), 184.2 (s, CO acac), 163.4 (d, $^{2}J_{C-F}$ = 6.5, Cq), 152.9 (s, NCN), 150.8 (d, $^{2}J_{C-F}$ = 7.2, Cq), 147.8 (s, CH), 142.6 (s, Cq) 138.5 (s, CH), 134.1 (s, CH), 129.6 (br, Cq), 125.6 (s, Cq), 125.1 (s, CH), 123.6 (d, $^{4}J_{C-F}$ = 20.9, CH), 122.5 (s, CH), 122.3 (s, CH), 121.6 (s, CH), 120.1 (dd, d, $^{2}J_{C-F}$ = 16.4, $^{4}J_{C-F}$ = 2.8, CH), 115.0 (s, CH), 111.1 (s, CH), 101.1 (s, CH acac), 97.2 (dd, $^{2}J_{C-F}$ = 27.3, $^{2}J_{C-F}$ = 27.3, CH), 35.5 (s, NCH_3), 28.6 and 28.4 (both s, CH_3 acac). A CF resonance is not observed due to low solubility of the complex. $^{19}F\{^{1}H\}$ NMR (282.33 MHz, CD_2Cl_2, 298 K): δ -111.0 (d, $^{4}J_{F-F}$ = 9.7, 1F, CF), -111.4 (d, $^{4}J_{F-F}$ = 9.7, 1F, CF).

Preparation of [Ir{κ^2-*C*,*C*-(C_6H_4-ImMe)}{κ^2-*C*,*N*-(C_6H_4-isoqui)}(H_2O)$_2$]X (X = BF_4 (9a[BF_4]), OTf (9a[OTf])). A red solution of **6a** (1.04 g, 1.59 mmol) in acetone (27 mL) in the presence of water (8.6 mL, 477.25 mmol), was treated with HBF_4·Et_2O (1.53 mL, 11.15 mmol) or CF_3SO_3H (1.01 mL, 11.15 mmol). After stirring for 24 h at room temperature, the resulting orange solution was filtered through celite and evaporated under vacuum to eliminate acetone, obtaining a red oil and a supernatant water solution. The water solution was removed via cannula and diethyl ether (20 mL) was added to afford an oil, that was washed with further portions of diethyl ether (2 × 10 mL), and dried in vacuo, obtaining **9a[BF_4]** or **9a[OTf]** as dark orange solids. **9a[BF_4]**: Yield: 719 mg (67%). Anal. Calcd. for $C_{25}H_{23}BF_4IrN_3O_2$: C, 44.39; H, 3.43; N, 6.21. Found: C, 44.96; H, 3.43; N, 5.39. ESIMS (electrospray, *m/z*) calcd for $C_{25}H_{19}IrN_3$ [M -

$2H_2O]^+$: 554.1; found: 554.1. ^{1}H NMR (500.13 MHz, CD_2Cl_2, 298 K): δ 8.90 (m, 1H, CH), 8.85 (m, 1H, CH), 8.12 (m, 1H, CH), 8.07 (m, 1H, CH), 7.87-7.84 (m, 2H, CH), 7.78 (m, 1H, CH), 7.55 (br, 1H, CH), 7.23 (br, 1H, CH), 7.02 (m, 1H, CH), 6.95 (m, 1H, CH), 6.80-6.75 (m, 2H, CH), 6.45-6.35 (m, 2H, CH), 5.85 (m, 1H, CH), 4.40-3.90 (br, H_2O), 4.06 (s, 3H, NCH_3). $^{13}C\{^1H\}$ + HMBC + HSQC NMR (125.76 MHz, CD_2Cl_2, 298 K): δ 166.8 (Cq), 161.8 (NCN), 153.9 (Cq), 146.2 (Cq), 139.6 (CH), 138.5 (Cq), 138.1 (CH), 134.3 (CH), 132.0 (CH), 130.6 (CH), 130.3 (CH), 128.9 (CH), 128.1 (CH), 127.5 (CH), 126.6 (Cq), 124.7 (CH), 123.3 (CH), 122.8 (CH), 122.3 (CH), 121.7 (CH), 115.6 (CH), 111.2 (CH), 36.3 (NCH_3). **9a[OTf]**: Yield: 705 mg (60%). X-ray quality crystals were grown by slow evaporation of a dichloromethane solution of this complex at room temperature.

Optimization of the Ratio 9a:2-(2-pinacolborylphenyl)-5-methylpyridine. An orange solution of **9a[BF_4]** (14 mg, 0.02 mmol) in 2–propanol (1 mL) was treated with K_3PO_4 (21.2 mg, 0.1 mmol) and different amounts of 2-(2-pinacolborylphenyl)-5-methylpyridine (5.9 mg, 0.1 mmol; 29.5 mg, 0.02 mmol; 59 mg, 0.2 mmol; 88.5 mg, 0.3 mmol). After 24 h stirring at room temperature, the resulting dark-orange solution was dried under vacuum, dissolved in CD_2Cl_2, and analyzed by ^{1}H NMR spectroscopy.

Optimization of the Ratio 9a:K_3PO_4. An orange solution of **9a[BF_4]** (14 mg, 0.02 mmol) in 2-propanol (1 mL) was treated with 2-(2-pinacolborylphenyl)-5-methylpyridine (6 mg, 0.02 mmol) and different amounts of K_3PO_4 (21.2 mg, 0.1 mmol; 42.4 mg, 0.2 mmol; 84.5 mg, 0.4 mmo; 169.8 mg, 0.8 mmol). After 24 h stirring at room temperature, the resulting dark-orange solution was dried under vacuum, dissolved in CD_2Cl_2, and analyzed by ^{1}H NMR spectroscopy.

Preparation of Ir{κ^2-*C*,*C*-(C_6H_4-ImMe)}{κ^2-*C*,*N*-(C_6H_4-isoqui)}{κ^2-*C*,*N*-(C_6H_4-Mepy)} (10a). An orange solution of **9a[BF_4]** (920 mg, 1.44 mmol) in 2-propanol (60 mL) was treated with K_3PO_4 (12.2 g, 57.48 mmol) and 2-(2-pinacolborylphenyl)-5-methylpyridine (0.424 mg, 1.44 mmol). After 48 h stirring at room temperature, the resulting red suspension was filtered through Celite, and the Celite extracted with dichloromethane (150 mL) to afford a red solution that was evaporated to dryness, affording a red solid. The solid was recrystallized by diffusion of pentane into a concentrated solution of the solid in dichloromethane. Yield: 650 mg (66%). X-ray quality crystals were grown by layering a solution of this complex in CH_2Cl_2 with pentane. Anal. Calcd. for $C_{37}H_{29}IrN_3$: C, 61.48; H, 4.18; N, 7.75. Found: C, 61.03; H, 4.48; N, 7.95. ESIMS (electrospray, *m/z*) calcd for $C_{37}H_{29}IrN_4$ $[M]^+$: 722.20; found: 722.40. ^1H NMR (500 MHz, CD_2Cl_2, 298 K): δ 8.93 (m, 1H, CH), 8.22 (m, 1H, CH), 7.83-7.74 (m, 4H, CH), 7.69-7.63 (m, 2H, CH), 7.61 (m, 1H, CH), 7.41-7.39 (m, 2H, CH), 7.15-7.05 (m, 4H, CH), 7.00-6.97 (m, 2H, CH), 6.91-6.88 (m, 1H, CH), 6.83-6.76 (m, 3H, CH), 6.50 (m, 1H, CH), 6.08 (m, 1H, CH), 2.98 (s, 3H, NCH_3), 1.98 (s, 3H, CH_3). $^{13}C\{^1H\}$ + HMBC + HSQC NMR (125.76 MHz, CD_2Cl_2, 298 K): δ 178.6 (Cq), 173.6 (Cq), 170.6 (Cq), 166.8 (Cq), 164.5 (NCN), 152.0 (CH), 147.0 (Cq), 146.5 (Cq), 146.4 (Cq), 143.7 (CH), 142.8 (Cq), 138.7 (CH), 137.9 (CH), 137.4 (CH), 137.0 (Cq), 132.5 (CH), 131.9 (Cq), 131.4 (CH), 130.7 (CH), 130.3 (CH), 129.7 (CH), 128.3 (CH), 127.6 (CH), 127.3 (CH), 126.8 (Cq), 124.5 (CH), 124.2 (CH), 121.3 (CH), 121.2 (CH), 120.4 (CH), 119.4 (CH), 118.6 (CH), 113.9 (CH), 110.4 (CH), 35.4 (NCH_3), 18.2 (CH_3).

Preparation of Ir{κ^2-*C*,*C*-(C_6H_4-ImMe)}{κ^2-*C*,*N*-(C_6H_4-isoqui)}{κ^2-*C*,*N*-(C_6H_4-Mepy)} (10a'). An orange solution of **9a[BF_4]** (150 mg, 0.22 mmol) in 2-propanol (5 mL) was treated with K_3PO_4 (233 mg, 1.1 mmol) and 2-(2-pinacolborylphenyl)-5-methylpyridine (65 mg, 0.22 mmol). After 24 h stirring at room temperature, the resulting dark-orange solution was dried

under vacuum. The resulting residue was dissolved in the minimal amount of dichloromethane and loaded onto a silica gel column (230-400 mesh). The column was eluted with ethylacetate/hexane/toluene 0.1/2/0.2 yielding **10a** (red) and **10a'** (red).Yield: **10a**: 48 mg (30%), **10a'**: 22 mg (14%). Spectroscopic data of isomer **10a'**: ESIMS (electrospray, *m/z*) calcd for $C_{37}H_{29}IrN_4$ $[M]^+$: 722.20; found: 722.40. ^{1}H NMR (300 MHz, CD_2Cl_2, 298 K): δ 8.94 (m, 1H, CH), 8.22 (m, 1H, CH), 7.88 (m, 1H, CH), 7.80–7.76 (m, 2H, CH), 7.72–7.66 (m, 4H, CH), 7.46–7.41 (m, 2H, CH), 7.39 (m, 1H, CH), 7.11 (m, 1H, CH), 6.98–6.93 (m, 2H, CH), 6.90–6.87 (m, 3H, CH), 6.83 (m, 1H, CH), 6.78–6.76 (m, 2H, CH), 6.60 (m, 1H, CH), 6.30 (m, 1H, CH), 2.95 (s, 3H, CH_3), 2.04 (s, 3H, CH_3). $^{13}C\{^1H\}$ + HMBC + HSQC NMR (75 MHz, CD_2Cl_2, 298 K): δ 174.8 (Cq), 173.3 (Cq), 169.3 (Cq), 166.8 (Cq), 166.7 (NCN), 152.0 (CH), 151.2 (CH), 146.5 (Cq), 145.8 (Cq), 143.1 (Cq), 138.4 (CH), 138.0 (CH), 137.4 (CH), 132.2 (CH), 132.1 (Cq), 131.8 (Cq), 129.8 (CH), 129.7 (CH), 124.5 (CH), 124.4 (CH), 124.1 (CH), 121.2 (CH), 121.0 (CH), 120.8 (CH), 120.1 (CH), 119.5 (CH), 119.4 (CH), 118.8 (CH), 118.7 (CH), 113.8 (CH), 110.3 (CH), 35.4 (NCH_3), 18.2 (CH_3).

ASSOCIATED CONTENT

Supporting Information

The Supporting Information is available free of charge on the ACS publications web site.

General information, crystallographic data, computational details, NMR spectra, experimental and computed UV/vis spectra, frontier molecular orbitals, normalized excitation and emission spectra, and cyclic voltammograms (PDF)

Cartesian coordinates of the optimized structures (XYZ).

Accession codes

CCDC 1585742-1585745 and 1836772-1836773 contain the crystallographic data for this paper. These data can be obtained free of charge *via* www.ccdc.cam.ac.uk/data_request/cif, or by e-mailing data_request@ccdc.cam.ac.uk, or by contacting The Cambridge Crystallographic Data Centre, 12 Union Road, Cambridge CB2 1EZm UK; fax: +44 1223 336033.

AUTHOR INFORMATION

Corresponding Author

* E-mail: maester@unizar.es.

Author Contributions

The manuscript was written through contributions of all authors. All authors have given approval to the final version of the manuscript.

Notes

The authors declare no competing financial interest.

ACKNOWLEDGMENTS

Financial support from the MINECO of Spain (Projects CTQ2017-82935-P and Red de Excelencia Consolider CTQ2016-81797-REDC), the Diputación General de Aragón (E06_17R), FEDER, and the European Social Fund is acknowledged.

REFERENCES

(1) (a) You, Y.; Park, Y. Phosphorescent iridium(III) complexes: toward high phosphorescence quantum efficiency through ligand control. *Dalton Trans.* **2009**, 1267-1282. (b) Chi, Y.; Chou,

P.-T. Transition-metal phosphors with cyclometalating ligands: fundamentals and applications. *Chem. Soc. Rev.* **2010**, *39*, 638-655. (c) Chou, P.-T.; Chung, M.-W.; Lin, C.-C. Harvesting luminescence via harnessing the photophysical properties of transition metal complexes. *Coord. Chem. Rev.* **2011**, *255*, 2653-2665. (d) Yersin, H.; Rausch, A. F.; Czerwieniec, R.; Hofbeck, T.; Fischer, T. The triplet state of organo-transition metal compounds. Triplet harvesting and singlet harvesting for efficient OLEDs. *Coord. Chem. Rev.* **2011**, *255*, 2622-2652. (e) Zanoni, K. P. S.; Coppo, R. L.; Amaral, C. R.; Iha, N. Y. M. Ir(III) complexes designed for light-emitting devices: beyond the luminescence color array. *Dalton Trans.* **2015**, *44*, 14559-14573. (f) Lu, C.W.; Wang, Y.; Chi, Y. Metal Complexes with Azolate-Functionalized Multidentate Ligands: Tactical Designs and Optoelectronic Applications. *Chem Eur. J.* **2016**, *22*, 17892-27908.

(2) See for example: Baranoff, E.; Curchod, B. F. E.; Frey, J.; Scopelliti, R.; Kessler, F.; Tavernelli, I.; Rothlisberger, U.; Grätzel, M.; Nazeeruddin, Md. K. Acid-Induced Degradation of Phosphorescent Dopants for OLEDs and Its Application to the Synthesis of Tris-heteroleptic Iridium(III) Bis-cyclometalated Complexes. *Inorg. Chem.* **2012**, *51*, 215-224.

(3) Costa, R. D.; Ortí, E.; Bolink ; H. J.; Monti, F.; Accorsi, G.; Armaroli, N. Luminescent Ionic Transition-Metal Complexes for Light-Emitting Electrochemical Cells. *Angew. Chem. Int. Ed.* **2012**, *51*, 8178-8211.

(4) Atwood, J. D., *Inorganic and Organometallic Reaction Mechanisms*; VCH Publishers: New York, 1997; Chapter 3.

(5) For recent examples see: (a) Lin, J.; Chau, N.-Y.; Liao, J.-L.; Wong, W.-Y.; Lu, C.-Y.; Sie, Z.-T.; Chang, C.-H.; Fox, M. A.; Low, P. J.; Lee, G.-H.; Chi, Y. Bis-Tridentate Iridium(III) Phosphors Bearing Functional 2‑Phenyl-6-(imidazol-2-ylidene)pyridine and 2‑(Pyrazol-3-yl)-6-

phenylpyridine Chelates for Efficient OLEDs. *Organometallics* **2016**, *35*, 1813-1824. (b) Axtell, J. C.; Kirlikovali, K. O.; Djurovich, P. I.; Jung, D.; Nguyen, V. T.; Munekiyo, B.; Royappa, A. T.; Rheingold, A. L.; Spokoyny, A. M. Blue Phosphorescent Zwitterionic Iridium(III) Complexes Featuring Weakly Coordinating nido-Carborane-Based Ligands. *J. Am. Chem. Soc.* **2016**, *138*, 15758-15765. (c) Esteruelas, M. A.; Oñate, E.; Palacios, A. U. Selective Synthesis and Photophysical Properties of Phosphorescent Heteroleptic Iridium(III) Complexes with Two Different Bidentate Groups and Two Different Monodentate Ligands. *Organometallics* **2017**, *36*, 1743-1755. (d) Kuo, H.H.; Chen, Y.-T.; Devereux, L. R.; Wu, C.-C.; Fox, M. A.; Kuei, C.-Y.; Chi, Y.; Lee, G.-H. Bis-Tridentate Ir(III) Metal Phosphors for Efficient Deep-Blue Organic Light-Emitting Diodes. *Adv. Mater.* **2017**, *29*, 1702464. (e) Esteruelas, M. A.; Gómez-Bautista, D.; López, A. M.; Oñate, E.; Tsai, J.-Y.; Xia, C. η^1-Arene Complexes as Intermediates in the Preparation of Molecular Phosphorescent Iridium(III) Complexes. *Chem. Eur. J.* **2017**, *23*, 15729-15737.

(6) (a) You, Y.; Nam, W. Photofunctional triplet excited states of cyclometalated Ir(III) complexes: beyond electroluminescence. *Chem. Soc. Rev.* **2012**, *41*, 7061-7084. (b) Omae, I. Application of the five-membered ring blue light-emitting iridium products of cyclometalation reactions as OLEDs. *Coord. Chem. Rev.* **2016**, *310*, 154-169. (c) Kapturkiewicz, A. Cyclometalated iridium(III) chelates-a new exceptional class of the electrochemiluminescent luminophores. *Anal. Bioanal. Chem.* **2016**, *408*, 7013-7033. (d) Chi, Y.; Chang, T.-K.; Ganesan, P.; Rajakannu, P. Emissive bis-tridentate Ir(III) metal complexes: Tactics, photophysics and applications. *Coord. Chem. Rev.* **2017**, *346*, 91-100.

(7) (a) Hu, T.; He, L.; Duan, L.; Qiu, Y. Solid-state light-emitting electrochemical cells based on ionic iridium(III) complexes. *J. Mat. Chem.* **2012**, *22*, 4206-4215. (b) Suhr, K. J.; Bastatas, L.

D.; Shen, Y.; Mitchell, L. A.; Fraizer, G. A.; Taylor, D. W.; Slinker, J. D.; Holliday, B. J. Phenyl substitution of cationic bis-cyclometalated iridium(III) complexes for iTMC-LEECs. *Dalton Trans.* **2016**, *45*, 17807-17823.

(8) (a) Felici, M.; Contreras-Carballada, P.; Smits, J. M. M.; Nolte, R. J. M.; Williams, R. M.; De Cola, L.; Feiters, M. Cationic Heteroleptic Cyclometalated Iridium^{III} Complexes Containing Phenyl-Triazole and Triazole-Pyridine Clicked Ligands. *Molecules* **2010**, *15*, 2039-2059. (b) Tordera, D.; Delgado, M.; Ortí, E.; Bolink, H. J.; Frey, J.; Nazeeruddin, Md. K.; Baranoff, E. Stable Green Electroluminescence from an Iridium Tris-Heteroleptic Ionic Complex. *Chem. Mater.* **2012**, *24*, 1896-1903. (c) Tordera, D.; Serrano-Pérez, J. J.; Pertegás, A.; Ortí, E.; Bolink, H. J.; Baranoff, E.; Nazeeruddin, Md. K.; Frey, J. Correlating the Lifetime and Fluorine Content of Iridium(III) Emitters in Green Light-Emitting Electrochemical Cells. *Chem. Mater.* **2013**, *25*, 3391-3397. (d) Lepeltier, M.; Graff, B.; Lalevée, J.; Wantz, G.; Ibrahim-Ouali, M.; Gigmes, D.; Dumur, F. Heteroleptic iridium (III) complexes with three different ligands: Unusual triplet emitters for light-emitting electrochemical cells. *Org. Electron.* **2016**, *37*, 24-34.

(9) (a) Brulatti, P.; Gildea, R. J.; Howard, J. A. K.; Fattori, V.; Cocchi, M.; Williams, G. Luminescent Iridium(III) Complexes with N^C^N-Coordinated Terdentate Ligands: Dual Tuning of the Emission Energy and Application to Organic Light-Emitting Devices. *Inorg. Chem.* **2012**, *51*, 3813-3826. (b) Alabau, R. G., Eguillor, B.; Esler, J.; Esteruelas, M. A.; Oliván, M.; Oñate, E.; Tsai, J.-Y.; Xia, C. CCC–Pincer–NHC Osmium Complexes: New Types of Blue-Green Emissive Neutral Compounds for Organic Light-Emitting Devices (OLEDs). *Organometallics* **2014**, *33*, 5582-5596. (c) Duan, T.; Chang, T.-K.; Chi, Y.; Wang, J.-Y., Chen, Z.-N.; Hung, W.-Y.; Chen, C.-H.; Lee, G.-H. Blue-emitting heteroleptic Ir(III) phosphors with functional 2,3'-bipyridine or 2-(pyrimidin-5-yl)-pyridine cyclometalates. *Dalton Trans.* **2015**, *44*, 14613-14624.

(d) Jou, J.-H.; Kumar, S.; Agrawal, A.; Li, T.-H.; Sahoo, S. Approaches for fabricating high efficiency organic light emitting diodes. *J. Mater. Chem. C.* **2015**, 3, 2974-3002. (e) Xu, Q.-L.; Liang, X.; Jiang, L.; Zhao, Y.; Zheng, Y.-X. Crystal structure, photoluminescence and electroluminescence of three bluish green light-emitting iridium complexes. *Dalton Trans.* **2016**, *45*, 7366-7372. (f) Umamahesh, B.; Karthikeyan, N. S.; Sathiyanarayanan, K. I.; Malicka, J. M.; Cocchi, M. Tetrazole iridium(III) complexes as a class of phosphorescent emitters for high-efficiency OLEDs. *J. Mater. Chem. C* **2016**, *4*, 10053-10060. (g) Benjamin, H.; Liang, J.; Liu, Y.; Geng, Y.; Liu, X.; Zhu, D.; Batsanov, A. S.; Bryce, M. R. Color Tuning of Efficient Electroluminescence in the Blue and Green Regions Using Heteroleptic Iridium Complexes with 2‑Phenoxyoxazole Ancillary Ligands. *Organometallics* **2017**, *36*, 1810-1821.

(10) (a) Stringer, B. D.; Quan, L. M.; Barnard, P. J.; Wilson, D. J. D.; Hogan, C. F. Iridium Complexes of N‑Heterocyclic Carbene Ligands: Investigation into the Energetic Requirements for Efficient Electrogenerated Chemiluminescence. *Organometallics* **2014**, *33*, 4860-4872. (b) Kim, T.; Lee, J.; Lee, S. U.; Lee, M. H. *o*‑Carboranyl–Phosphine as a New Class of Strong-Field Ancillary Ligand in Cyclometalated Iridium(III) Complexes: Toward Blue Phosphorescence. *Organometallics* **2015**, *34*, 3455-3458. (c) Lee, Y. H.; Park, J.; Lee, J.; Lee S. U.; Lee, M. H. Iridium Cyclometalates with Tethered o‑Carboranes: Impact of Restricted Rotation of *o*‑Carborane on Phosphorescence Efficiency. *J. Am. Chem. Soc.* **2015**, *137*, 8018-8021. (d) Li, T.-Y.; Liang, X.; Zhou, L.; Wu, C.; Zhang, S.; Liu, X.; Lu, G.-Z.; Xue; L.-S.; Zheng, Y. X.; Zuo, J.-L. *N*‑Heterocyclic Carbenes: Versatile Second Cyclometalated Ligands for Neutral Iridium(III) Heteroleptic Complexes. *Inorg. Chem.* **2015**, *54*, 161-173. (e) Nguyen, V. H.; Khoo, R. S. H.; Yip, J. H. K. Ir(2-Phenylpyridine)$_2$(benzene-1,2-dithiolate) Anion as a Diastereoselective

Metalloligand and Nucleophile: Stereoelectronic Effect, Spectroscopy, and Computational Study of the Methylated and Aurated Complexes and their Oxygenation Products. *Inorg. Chem*. **2015**, *54*, 2264-2277. (f) Radwan, Y. K.; Maity, A.; Teets, T. Manipulating the Excited States of Cyclometalated Iridium Complexes with β-Ketoiminate and β-Diketiminate Ligands. *Inorg. Chem.* **2015**, *54*, 7122-7131. (g) Kumar, S.; Hisamatsu, Y.; Tamaki, Y.; Ishitani, O.; Aoki, S. Design and Synthesis of Heteroleptic Cyclometalated Iridium(III) Complexes Containing Quinoline-Type Ligands that Exhibit Dual Phosphorescence. *Inorg. Chem.* **2016**, *55*, 3829-3843. (h) Yi, S.; Kim, J.-H.; Cho, Y.-J.; Lee, J.; Choi, T.-S.; Cho, D. W.; Pac, C.; Han, W.-S.; Son, H.-J.; Kang, S. O. Stable Blue Phosphorescence Iridium(III) Cyclometalated Complexes Prompted by Intramolecular Hydrogen Bond in Ancillary Ligand. *Inorg. Chem.* **2016**, *55*, 3324-3331. (i) Jing, Y.-M.; Zhao, Y.; Zheng, Y.-X. Photoluminescence and electroluminescence of iridium(III) complexes with 2',6'-bis(trifluoromethyl)-2,4'-bipyridine and 1,3,4-oxadiazole/1,3,4-thiadiazole derivative ligands. *Dalton Trans.* **2017**, *46*, 845-853. (j) Benjamin, H.; Liang, J.; Liu, Y.; Geng, Y.; Liu, X.; Zhu, D.; Batsanov, A. S.; Bryce, M. R. Color Tuning of Efficient Electroluminescence in the Blue and Green Regions Using Heteroleptic Iridium Complexes with 2-Phenoxyoxazole Ancillary Ligands. *Organometallics* **2017**, *36*, 1810-1821. (k) Pal, A. K.; Henwood, A. F.; Cordes, D. B.; Slawin, A. M. Z.; Samuel, I. D. W.; Zysman-Colman, E. Blue-to-Green Emitting Neutral Ir(III) Complexes Bearing Pentafluorosulfanyl Groups: A Combined Experimental and Theoretical Study. *Inorg. Chem.* **2017**, *56*, 7533-7544.

(11) (a) Edkins, R. M.; Wriglesworth, A.; Fucke, K.; Bettington, S. L.; Beeby, A. The synthesis and photophysics of tris-heteroleptic cyclometalated iridium Complexes. *Dalton Trans.* **2011**, *40*, 9672-9678. (b) Xu, X.; Yang, X.; Dang, J.; Zhou, G.; Wu, Y.; Li, H.; Wong, W.-Y. Trifunctional Ir^{III} ppy-type asymmetric phosphorescent emitters with ambipolar features for

highly efficient electroluminescent devices. *Chem. Commun.* **2014**, *50*, 2473-2476. (c) Lepeltier, M.; Dumur, F.; Graff, B.; Xiao, P.; Gigmes, D.; Lalevée, J.; Mayer, C. R. Tris-cyclometalated Iridium(III) Complexes with Three Different Ligands: a New Example with 2-(2,4-Difluorophenyl)pyridine-Based Complex. *Helv. Chim. Acta* **2014**, *97*, 939-956. (d) Xu, X.; Yang, X.; Wu, Y.; Zhou, G.; Wu, C.; Wong, W.-Y. *tris*-Heteroleptic Cyclometalated Iridium(III) Complexes with Ambipolar or Electron Injection/Transport Features for Highly Efficient Electrophosphorescent Devices. *Chem. Asian J.* **2015**, *10*, 252-262. (e) Tamura, Y.; Hisamatsu, Y.; Kumar, S.; Itoh, Y.; Kyouhei, S.; Kuroda, R.; Aoki, S. Efficient Synthesis of Tris-Heteroleptic Iridium(III) Complexes Based on the Zn^{2+}-Promoted Degradation of Tris-Cyclometalated Iridium(III) Complexes and Their Photophysical Properties. *Inorg. Chem.* **2017**, *56*, 812-833.

(12) (a) Hisamatsu, Y.; Kumar, S.; Aoki, S. Design and Synthesis of Tris-Heteroleptic Cyclometalated Iridium(III) Complexes Consisting of Three Different Nonsymmetric Ligands Based on Ligand-Selective Electrophilic Reactions via Interligand HOMO Hopping Phenomena. *Inorg. Chem.* **2017**, *56*, 886-899. (b) Tamura, Y.; Hisamatsu, Y.; Kazama, A.; Yoza, K.; Sato, K.; Kuroda, R.; Aoki. S. Stereospecific Synthesis of Tris-heteroleptic Tris-cyclometalated Iridium(III) Complexes via Different Heteroleptic Halogen-Bridged Iridium(III) Dimers and Their Photophysical Properties. *Inorg. Chem.* **2018**, *57*, 4571-4589.

(13) Cudré, Y.; Franco de Carvalho, F.; Burgess, G. R.; Male, L.; Pope, S. J. A.; Tavernelli, I.; Baranoff, E. Tris-heteroleptic Iridium Complexes Based on Cyclometalated Ligands with Different Cores. *Inorg. Chem.* **2017**, *56*, 11565-11576.

(14) Liao, J.-L.; Chi, Y.; Sie, Z.-T.; Ku, C.-H.; Chang, C.-H.; Fox, M. A.; Low, P. J.; Tseng, M.-R.; Lee, G.-H. Ir(III)-Based Phosphors with Bipyrazolate Ancillaries; Rational Design, Photophysics, and Applications in Organic Light-Emitting Diodes. *Inorg. Chem.* **2015**, *54*, 10811-10821.

(15) (a) Frenking, G.; Solá, M.; Vyboishchikov, S. Chemical bonding in transition metal carbene complexes. *J. Organomet. Chem.* **2005** *690*, 6178-6204. (b) Díez-González, S.; Nolan, S. P. Stereoelectronic parameters associated with N-heterocyclic carbene (NHC) ligands: A quest for understanding. *Coord. Chem. Rev.* **2007**, *251*, 874-883. (c) Jacobsen, H.; Correa, A.; Poater, A.; Costabile, C.; Cavallo, L. Understanding the M (NHC) (NHC = N-heterocyclic carbene) bond. *Coord. Chem. Rev.* **2009**, *253*, 687-703. (d) Nelson, D. J.; Nolan, S. P. Quantifying and understanding the electronic properties of *N*-heterocyclic carbenes. *Chem. Soc. Rev.* **2013**, *42*, 6723-6753.

(16) (a) Peris, E.; Crabtree, R. H. Recent homogeneous catalytic applications of chelate and pincer *N*-heterocyclic carbenes. *Coord. Chem. Rev.* **2004**, *248*, 2239-2246. (b) Kantchev, E. A. B.; O'Brien, C. J.; Organ, M. G. Palladium Complexes of N-Heterocyclic Carbenes as Catalysts for Cross-Coupling Reactions-A Synthetic Chemist's Perspective. *Angew. Chem. Int. Ed.* **2007**, *46*, 2768-2813. (c) Corberán, R.; Mas-Marzá, E.; Peris, E. Mono-, Bi- and Tridentate N-Heterocyclic Carbene Ligands for the Preparation of Transition-Metal-Based Homogeneous Catalysts. *Eur. J. Inorg. Chem.* **2009**, 1700-1716. (d) Díez-González, S.; Marion, N.; Nolan, S. P. N-Heterocyclic Carbenes in Late Transition Metal Catalysis. *Chem. Rev.* **2009**, *109*, 3612-3676. (e) Poyatos, M.; Mata, J. A.; Peris, E. Complexes with Poly(N-heterocyclic carbene) Ligands: Structural Features and Catalytic Applications. *Chem. Rev.* **2009**, *109*, 3677-3707. (f) Schuster, O.; Yang, L.; Raubenheimer, H. G.; Albrecht, M. Beyond Conventional *N*-Heterocyclic

Carbenes: Abnormal, Remote, and Other Classes of NHC Ligands with Reduced Heteroatom Stabilization. *Chem. Rev.* **2009**, *109*, 3445-3478. (g) Esteruelas, M. A.; López, A. M.; Oliván, M. Polyhydrides of Platinum Group Metals: Nonclassical Interactions and σ⁻Bond Activation Reactions. *Chem. Rev.* **2016**, *116*, 8770-8847. (h) Peris, E. Smart N-Heterocyclic Carbene Ligands in Catalysis. *Chem. Rev.* doi: 10.1021/acs.chemrev.6b00695.

(17) (a) Mercs, L.; Albrecht, M. Beyond catalysis: N-heterocyclic carbene complexes as components for medicinal, luminescent, and functional materials applications. *Chem. Soc. Rev.* **2010**, *39*, 1903-1912. (b) Visbal, R.; Gimeno, M. C. N-heterocyclic carbene metal complexes: photoluminescence and applications. *Chem. Soc. Rev.* **2014**, *43*, 3551-3574.

(18) Bolaño, T.; Esteruelas, M. A.; Fernández, I.; Oñate, E.; Palacios, A.; Tsai, J.-Y.; Xia, C. Osmium(II)-Bis(dihydrogen) Complexes Containing C_{aryl},C_{NHC}-Chelate Ligands: Preparation, Bonding Situation, and Acidity. *Organometallics* **2015**, *34*, 778-789.

(19) (a) Chang, C.-F.; Cheng, Y.-M.; Chi, Y.; Chiu, Y.-C.; Lin, C.-C.; Lee, G.-H.; Chou, P.-T.; Chen, C.-C.; Chang, C.-H.; Wu, C.-C. Highly Efficient Blue-Emitting Iridium(III) Carbene Complexes and Phosphorescent OLEDs. *Angew. Chem. Int. Ed.* **2008**, *47*, 4542-4545. (b) Chien, C.-H.; Fujita, S.; Yamamoto, S.; Hara, T.; Yamagata, T.; Watanabe, M.; Mashima, K. Stepwise and one-pot syntheses of Ir(III) complexes with imidazolium-based carbene ligands. *Dalton Trans.* **2008**, 916-923. (c) Tsurugi, H.; Fujita, S.; Choi, G.; Yamagata, T.; Ito, S.; Miyasaka, H.; Mashima, K. Carboxylate Ligand-Induced Intramolecular C-H Bond Activation of Iridium Complexes with *N*-Phenylperimidine-Based Carbene Ligands. *Organometallics* **2010**, *29*, 4120-4129. (d) Hsieh, C.-H.; Wu, F.-L.; Fan, C.-H.; Huang, M.-J.; Lu, K.-Y.; Chou, P.-Y.; Ou Yang, Y.-H.; Wu, S.-H.; Chen, I.-C.; Chou, S.-H.; Wong, K.-T.; Cheng, C.-H. Design and Synthesis of

Iridium Bis(carbene) Complexes for Efficient Blue Electrophosphorescence. *Chem. Eur. J.* **2011**, *17*, 9180-9187. (e) Lu, K.-Y.; Chou, H.-H.; Hsieh, C.-H.; Ou Yang, Y.-H.; Tsai, H.-R.; Tsai, H.-Y.; Hsu, L.-C.; Chen, C.-Y.; Chen, I-C.; Cheng, C.-H. Wide-Range Color Tuning of Iridium Biscarbene Complexes from Blue to Red by Different N^N Ligands: an Alternative Route for Adjusting the Emission Colors. *Adv. Mater.* **2011**, *23*, 4933-4937. (f) Zhou, Y.; Jia, J.; Li, W.; Fei, H.; Zhou, M. Luminescent biscarbene iridium(III) complexes as living cell imaging reagents. *Chem. Commun.* **2013**, *49*, 3230-3232. (g) Li, H.; Yin, Y.-M.; Cao, H.-T.; Sun, H.-Z.; Wang, L.; Shan, G.-G.; Zhu, D.-X.; Su, Z.-M.; Xie, W.-F. Efficient greenish-blue phosphorescent iridium(III) complexes containing carbene and triazole chromophores for organic light-emitting diodes. *J. Organomet. Chem.* **2014**, *753*, 55-62. (h) Shang, X.; Han, D.; Zhan, Q.; Zhang, G.; Li, D. DFT and TD-DFT Study on the Electronic Structures and Phosphorescent Properties of a Series of Heteroleptic Iridium(III) Complexes. *Organometallics* **2014**, *33*, 3300-3308. (i) Esteruelas, M. A.; López, A. M.; Oñate, E.; San-Torcuato, A.; Tsai, J.-Y.; Xia, C. Preparation of Phosphorescent Iridium(III) Complexes with a Dianionic C,C,C,C-Tetradentate Ligand. *Inorg. Chem*. **2018**, *57*, 3720-3730.

(20) Albrecht, M. Cyclometalation Using d-Block Transition Metals: Fundamental Aspects and Recent Trends. *Chem. Rev.* **2010**, *110*, 576-623.

(21) Newman, C. P.; Clarkson, G. J.; Rourke, J. P. Silver(I) N-heterocyclic carbene halide complexes: A new bonding motif. *J. Organomet. Chem.* **2007**, *692*, 4962-4968.

(22) Hudson, Z. M.; Blight, B. A.; Wang, S. Efficient and High Yield One-Pot Synthesis of Cyclometalated Platinum(II) *β*-Diketonates at Ambient Temperature. *Org. Lett.* **2012**, *14*, 1700-1703.

(23) Chianese, A. R.; Kovacevic, A.; Zeglis, B. M.; Faller, J. W.; Crabtree, R. H. Abnormal C5-Bound N-Heterocyclic Carbenes: Extremely Strong Electron Donor Ligands and Their Iridium(I) and Iridium(III) Complexes. *Organometallics* **2004**, *23*, 2461-2468.

(24) Esteruelas, M. A.; Oñate, E.; Palacios, A.; Tsai, J.-Y.; Xia, C. Preparation of Capped Octahedral $OsHC_6$ Complexes by Sequentia-Carbon-Directed C–H Bond Activation Reactions. *Organometallics* **2016**, *35*, 2532-2542.

(25) Esteruelas, M. A.; Fernández-Alvarez, F. J.; Oliván, M.; Oñate, E. NH-Tautomerization of Quinolines and 2-Methylpyridine Promoted by a Hydride-Iridium(III) Complex: Importance of the Hydride Ligand. *Organometallics* **2009**, *28*, 2276-2284 and references therein.

(26) Esteruelas, M. A.; López, A. M.; Oñate, E.; San-Torcuato, A.; Tsai, J.-Y.; Xia, C. Formation of Dinuclear Iridium Complexes by NHC-Supported C–H Bond Activation. *Organometallics* **2017**, *36*, 699-707.

(27) Maity, A.; Anderson, B. L.; Deligonula, N.; Gray, T. G. Room-temperature synthesis of cyclometalated iridium(III) complexes: kinetic isomers and reactive functionalities. *Chem. Sci.* **2013**, *4*, 1175-1181.

(28) Zanoni, K. P. S.; Kariyazaki, B. K., Ito, A.; Brennaman, M. K.; Meyer, T. J.; Murakami Iha, N. Y. Blue-Green Iridium(III) Emitter and Comprehensive Photophysical Elucidation of Heteroleptic Cyclometalated Iridium(III) Complexes. *Inorg. Chem.* **2014** *53*, 4089-4099.

(29) (a) Su, Y.-J.; Huang, H.-L.; Li, C.-L.; Chien, C.-H.; Tao, Y.-T.; Chou, P.-T.; Datta, S.; Liu, R.-S. Highly Efficient Red Electrophosphorescent Devices Based on Iridium Isoquinoline Complexes: Remarkable External Quantum Efficiency Over a Wide Range of Current. *Adv.*

Mater **2003**, *15*, 884-888. (b) Bronstein, H. A.; Finlayson, C. E;. Kirov, K. R.; Friend, R. H.; Williams, C. K. Investigation into the Phosphorescence of a Series of Regioisomeric Iridium(III) Complexes. *Organometallics* **2008**, *27*, 2980-2989.

(30) Lamansky, S.; Djurovich, P.; Murphy, D.; Feras, A.-R.; Kwong, R.; Irina, T.; Bortz, M.; Mui, B.; Bau, R.; Thompson M. E. Synthesis and Characterization of Phosphorescent Cyclometalated Iridium Complexes. *Inorg. Chem.* **2001,** *40,* 1704-1711.

(31). Scholz, S.; Kondakov, D.; Lüssem, B.; Leo, K. Degradation Mechanisms and Reactions in Organic Light-Emitting Devices. *Chem. Rev*. **2015**, *115*, 8449−8503.

(32) van der Ent, A.; Onderdelinden, A. L. Schunn R. A. Chlorobis(Cyclooctene)Rhodium(I) and–Iridium(I) Complexes. *Inorg. Synth.* **1997**, *28*, 90-92.

(33) Monti, F.; La Placa, M. G. I.; Armaroli, N.; Scopelliti, R.; Grätzel, M.; Nazeeruddin, M. K.; Kessler, F. Cationic Iridium(III) Complexes with Two Carbene-Based Cyclometalating Ligands: Cis Versus Trans Isomers. *Inorg. Chem.* **2015**, *54*, 3031-3042.

SYNOPSIS

Efficient procedures to synthetize new families of neutral phosphorescent heteroleptic Ir(III) emitters bearing three different chelate ligands, namely, a cyclometalated aryl-NHC, a cyclometalated aryl-N-heterocycle, and an acac or a second cyclometalated aryl-N-heterocycle are discovered. The new complexes are stable to ligand redistribution processes and allow a color tuning in a wide range of emission wavelengths. The performance of an OLED device based on one of these complexes is included.

For Table of Contents Only